NUCLEAR MAGNETIC RESONANCE IN SINGLE CRYSTALS OF TIN AND ALUMINUM

by

EDWARD PETER JONES

B.A.Sc., University of British Columbia, 1958
M.Sc., University of British Columbia, 1959

A THESIS SUBMITTED IN PARTIAL FULFILMENT OF

THE REQUIREMENTS FOR THE DEGREE OF

DOCTOR OF PHILOSOPHY

in the Department

of

PHYSICS

We accept this thesis as conforming to the

required standard

THE UNIVERSITY OF BRITISH COLUMBIA

November, 1962

In presenting this thesis in partial fulfilment of the requirements for an advanced degree at the University of British Columbia, I agree that the Library shall make it freely available for reference and study. I further agree that permission for extensive copying of this thesis for scholarly purposes may be granted by the Head of my Department or by his representatives. It is understood that copying or publication of this thesis for financial gain shall not be allowed without my written permission.

Department of Physics

The University of British Columbia,
Vancouver 8, Canada.

Date January 7, 1963

ABSTRACT

Nuclear magnetic resonance studies in single crystals of aluminum and tin have been done at liquid helium temperatures. The Knight shift in tin has been studied as a function of crystal orientation in a constant magnetic field for different values of field and temperature. The anisotropic Knight shift in tin was observed directly for the first time. The line width of the tin resonance was also studied and found to depend on the crystal orientation in the magnetic field. The second moment of the line has been calculated in terms of dipole-dipole interactions and indirect exchange interactions between nuclei of different magnetic moments and compared with the experimental results.

The Knight shift was studied as a function of external field for both tin and aluminum in a search for de Haas-van Alphen type oscillations. No indication of these was found. An upper limit for this effect was determined for each sample.

ACKNOWLEDGMENT

I wish to express my sincere gratitude to Dr. Myer Bloom for the valuable instruction and inspiration he provided throughout my career as a graduate student, and for his support in obtaining financial assistance for my studies.

I wish also to express my gratitude to Dr. D. Ll. Williams for his help in the measurements reported in this work and for many useful suggestions particularly as regards work in single crystals.

My thanks are due to Dr. Roger Howard who introduced me to the IBM 1620 computer and who carried out the computation described in Chapter 4.

I wish to acknowledge the financial support provided by a fellowship given by the International Nickel Company of Canada and research funds made available by the National Research Council.

TABLE OF CONTENTS

LIST OF ILLUSTRATIONS

CHAPTER I

INTRODUCTION

The change in the nuclear magnetic resonance frequency of a nucleus in a metal from that of the same nucleus in a non-metallic state was first explained in terms of an electron-nucleus interaction by Townes, Herring and Knight[1]. This change in resonance frequency, the Knight shift, has been studied experimentally and theoretically quite extensively for many metals and alloys. The results of much of this work are summarized in a review article by Knight[2] and a rigorous theoretical treatment of the Knight shift is given by Abragam[3].

Because of the small skin depth of almost all metals, nuclear magnetic resonance experiments have been almost entirely confined to studies in metal powders whose individual particle sizes are less than the skin depth of the metal. In any metal with cubic symmetry, the Knight shift is independent of the orientation of the metal crystal with respect to the external magnetic field. However, if the symmetry of the crystal is less than cubic, this is not true. The nuclear magnetic resonance signal will be

broadened when observed in a powder whose particles are randomly oriented in the magnetic field or shifted when observed in a single crystal.

The purpose of this work has been to study the nuclear magnetic resonance in metal single crystals, in particular, white tin and aluminum.[31] The advantages of using a single crystal to study the nuclear magnetic resonance of tin are: (a) the anisotropy of the Knight shift due to the tetragonal symmetry of the tin crystal can be studied directly; (b) the line shape of the resonance can be studied without the large broadening caused by the anisotropic Knight shift; and (c) the measurements of the resonance frequency can be made more accurately because the resonance line is narrower.

The Sn^{117} and Sn^{119} isotopes were studied in a white tin single crystal as a function of crystal orientation in the magnetic field, as a function of the magnetic field itself, and as a function of temperature in the liquid helium range. The two parameters which describe the Knight shift in a metal with tetragonal symmetry were determined. A slight dependence of the Knight shift on temperature and external magnetic field was observed. The line width of the tin resonance was studied and found to have contributions from both the dipole-dipole interactions of nearest neighbours and from indirect exchange interactions which couple two nuclei of different magnetic moments by way of the conduction electrons.

A search for a variation of the Knight shift caused by oscillations in the diamagnetic susceptibility as the external field is varied (de Haas-van Alphen effect) was made in single crystals of both tin and aluminum. An upper limit to the effect has been set for both metals.

CHAPTER 2

THEORY OF THE KNIGHT SHIFT

The Knight shift in metals with tetragonal symmetry can be explained in terms of the hyperfine interaction which involves essentially three terms in the spin Hamiltonian and which couples the electron spins to the nuclear spins. The coupling energy is small compared to the atomic energy splittings so that perturbation theory can be used. Further, the electrons are assumed to be non-interacting, i.e., the free electron model is used.

The Hamiltonian for the magnetic interaction of the electrons with the nucleus can be written as[4]

$$(1)\quad \mathcal{H} = 2\beta\hbar\gamma\underline{I}\cdot\left[\frac{\underline{\ell}}{r^3} - \frac{\underline{S}}{r^3} + \frac{3\underline{r}\,(\underline{S}\cdot\underline{r})}{r^5} + \frac{8\pi}{3}\underline{S}\,\delta(r)\right]$$

where β is the Bohr magneton

γ is the nuclear gyromagnetic ratio

$\underline{I}$ is the nuclear spin

$\underline{\ell}$ is the electron orbital quantum number

$\underline{S}$ is the electron spin

$\underline{r}$ is the radius vector from the nuclear spin to the electron spin

The first term of this Hamiltonian will give almost no contribution to the electron-nucleus interaction in most metals because the orbital angular momentum is quenched or nearly so (bismuth is a notable exception). In other words, the diamagnetic contribution is usually small compared to the paramagnetic contribution. The diamagnetic contribution might be detected, however, by the observation of oscillations in the Knight shift at low temperatures as the magnetic field is varied. This point will be discussed in Chapter 5. For crystals with no lower than cubic symmetry, the second and third terms, the dipolar terms, of the Hamiltonian give no contribution to the Knight shift[5]. For crystals of tetragonal symmetry, they account for the anisotropic part of the Knight shift. The last term in the Hamiltonian couples only s-electrons to the nucleus and gives rise to the Knight shift in crystals of cubic symmetry or to the isotropic part of the Knight shift in crystals with tetragonal symmetry.

The standard derivation of the Knight shift is now given in detail following mainly the treatment given by Slichter[5]. This is being done for completeness. Since this work represents the first direct observation of the anisotropic contributions to the Knight shift, by giving this derivation the type of information obtainable in such an experiment should be more comprehensible.

For simplicity, first consider the interactions

involving only the last term, or the contact term, in the Hamiltonian

$$(2) \qquad \mathcal{H}_1 = \frac{16\pi}{3} \beta \gamma\hbar \, \underline{I} \cdot \underline{S} \, \delta(r)$$

Because the electrons and nuclei are only weakly interacting, the complete wave function Ψ can be approximated by the product of the many particle electronic and nuclear wave functions, Ψ_e and Ψ_n

$$\Psi = \Psi_e \Psi_n$$

The antisymmetrized electronic wave function is considered to be[6]

$$(3) \qquad \Psi_e = \frac{1}{\sqrt{N}} \sum_p (-1)^p \, \Psi_{\underline{k}s}(1) \, \Psi_{\underline{k}'s'}(2) \ldots \Psi_{\underline{k}^n s^n}(N)$$

where $\Psi_{\underline{k}\,s} = u_{\underline{k}} \, e^{i\underline{k}\cdot r} \, \Psi_s$, the Bloch function including the spin term, and p is an index to indicate an odd or even number of interchanges in the permutation.

The contribution of the electron-nuclear interactions from all electrons to one nucleus is

$$(4) \qquad \mathcal{H}_{1j} = \frac{16\pi}{3} \beta \gamma\hbar \, \underline{I}_j \cdot \int \Psi_e^* \sum_\ell \underline{S}_\ell \, \delta(r_\ell) \, \Psi_e \, d\tau_e$$

Since the operator $S_\ell \, \delta(r_\ell)$ involves only one electron, there are no contributions from terms in which electrons are exchanged. Thus using equation (3), we can rewrite (4)

$$(5) \quad \mathcal{H}_{1j} = \frac{16\pi}{3} \beta \gamma \hbar \, \underset{\sim}{I}_j \cdot \sum_\ell \int \left[\Psi_{\underset{\sim}{k}s}(1) \ldots \right]^* \underset{\sim}{S}_\ell \, \delta(r_\ell) \times \left[\Psi_{\underset{\sim}{k}s}(1) \ldots \right] d\tau_1 d\tau_2 \ldots$$

If the electrons are quantized along the z-direction by the external state field H_o, the only contribution to equation (5) comes from $S_{z\ell}$. The integral then becomes

$$(6) \quad \mathcal{H}_{1j} = \frac{16\pi}{3} \beta \gamma \hbar \, I_{zj} \sum_{\underset{\sim}{k},s} \left| u_{\underset{\sim}{k}}(o) \right|^2 m_s \, f(\underset{\sim}{k},s)$$

where the sum is over all $\underset{\sim}{k}$ and s, and $f(\underset{\sim}{k},s)$ is the Fermi distribution function giving the probability that a given state described by the wave vector $\underset{\sim}{k}$ and spin coordinate s is occupied. The factor m_s is just $+\frac{1}{2}$ or $-\frac{1}{2}$ and $u_{\underset{\sim}{k}}(o)$ is the spatial part of the electronic wave function evaluated at the nucleus. For a given $\underset{\sim}{k}$, equation (6) can be written

$$(7) \quad \mathcal{H}^{\underset{\sim}{k}}_{1j} = \frac{8\pi}{3} \gamma \hbar \, I_{zj} \left[2\beta(\tfrac{1}{2}) \, f(\underset{\sim}{k},\tfrac{1}{2}) + 2\beta(-\tfrac{1}{2}) \times f(\underset{\sim}{k},-\tfrac{1}{2}) \right] \left| u_{\underset{\sim}{k}}(o) \right|^2$$

The factor in square brackets is the average contribution of the $\underset{\sim}{k}$ state to the z component of magnetization of the sample. If this factor is called $\overline{\mu_{z\,\underset{\sim}{k}}}$, the total z magnetization of the electrons in a sample of a unit volume is $\overline{\mu_z}$

$$\overline{\mu_z} = \sum_{\underset{\sim}{k}} \overline{\mu_{z\,\underset{\sim}{k}}} \tag{8}$$

The total spin susceptibility for a unit volume can be defined as

$$\overline{\mu_z} = \chi_s H_o \tag{9}$$

and the spin susceptibility for one value of $\underset{\sim}{k}$

$$\overline{\mu_{z\,\underset{\sim}{k}}} = \chi^s_{\underset{\sim}{k}} H_o \tag{10}$$

which means that

$$\chi^s = \sum_{\underset{\sim}{k}} \chi^s_{\underset{\sim}{k}} \tag{10'}$$

The total effective interaction for the jth nuclear spin is then

$$\mathcal{H}_{1j} = \frac{-8\pi}{3} \gamma\hbar\, I_{zj} \left[\sum_{\underset{\sim}{k}} |u_{\underset{\sim}{k}}(o)|^2 \chi^s_{\underset{\sim}{k}} \right] H_o \tag{11}$$

In order that this sum may be evaluated, the following quantity must be considered. $g(E_{\underline{k}}, A)\, dE_{\underline{k}}\, dA$ is defined as the number of allowed $\underline{k}$-values lying within a small cylindrical volume of $\underline{k}$ space having a cross-section area dA and lying between the energy surfaces $E_{\underline{k}}$ and $E_{\underline{k}} + dE_{\underline{k}}$. The coordinates of the surface are denoted by A. The total number of states dN between $E_{\underline{k}}$ and $E_{\underline{k}} + dE_{\underline{k}}$ is given by summing the contributions over the whole constant energy surface.

$$dN = dE_{\underline{k}} \int_{E_{\underline{k}} = \text{const}} g(E_{\underline{k}}, A)\, dA \tag{12}$$

$$\equiv \rho(E_{\underline{k}})\, dE_{\underline{k}}$$

$\rho(E_{\underline{k}})$ is a density of states per unit energy interval at the energy surface $E_{\underline{k}}$ for a unit volume. For convenience later, $N(E_F)$ can be similarly defined as the density of states per unit energy interval at the Fermi surface for one atomic volume V_o. The sum in equation (11) can now be evaluated in terms of these quantities if the sum is replaced by an integral

$$\sum_{\underline{k}} |u_{\underline{k}}(o)|^2 \chi^s_{\underline{k}} = \int |u_{\underline{k}}(o)|^2 \chi^s_{\underline{k}}\, g(E_{\underline{k}}, A)\, dE_{\underline{k}}\, dA \tag{13}$$

$\chi^s_{\underline{k}}$ depends on the Fermi functions $f(\underline{k}, \frac{1}{2})$ and $f(\underline{k}, -\frac{1}{2})$ and on the difference in energy between two spins in the $\underline{k}$ state, one with spin parallel to the magnetic field and the other with spin antiparallel. Clearly, $\chi^s_{\underline{k}}$ will be the same for any states $\underline{k}$ having the same value of $E_{\underline{k}}$. It is therefore assumed that $\chi^s_{\underline{k}}$ can be written as a function only of the energy $E_{\underline{k}}$

$$\chi^s_{\underline{k}} = \chi^s (E_{\underline{k}}) \tag{14}$$

Equation (13) can now be written

$$\sum_{\underline{k}} |u_{\underline{k}}(o)|^2 \chi^s_{\underline{k}} = \int |u_{\underline{k}}(o)|^2 \chi^s (E_{\underline{k}}) \times g(E_{\underline{k}}, A)\, dA\, d E_{\underline{k}} \tag{15}$$

The average value of $|u_{\underline{k}}(o)|^2$ over a surface of constant energy is defined as

$$\langle |u_{\underline{k}}(o)|^2 \rangle_{E_{\underline{k}}} = \frac{\int |u_{\underline{k}}(o)|^2 g(E_{\underline{k}}, A)\, dA}{\int g(E_{\underline{k}}, A)\, dA} \tag{16}$$

$$= \frac{\int |u_{\underline{k}}(o)|^2 g(E_{\underline{k}}, A)\, dA}{\rho(E_{\underline{k}})}$$

so that

$$(17) \quad \sum_{\underline{k}} |u_{\underline{k}}(o)|^2 \chi^s_{\underline{k}} = \int \langle |u_{\underline{k}}(o)|^2 \rangle_{E_{\underline{k}}} \chi^s(E_{\underline{k}}) \times \rho(E_{\underline{k}}) \, dE_{\underline{k}}$$

Because the electron spins are either paired off or the electron spin energy states are unoccupied, for all $E_{\underline{k}}$ not near (not within a region of the order of kT) the Fermi surface E_F, the contributions of $\chi^s(E_{\underline{k}})$ to the total spin susceptibility will come only from energy states near the Fermi surface. If it is assumed that $\langle |u_{\underline{k}}(o)|^2 \rangle_{E_{\underline{k}}}$ varies slowly with $E_{\underline{k}}$, this in turn can be taken outside the integral

$$(18) \quad \sum_{\underline{k}} |u_{\underline{k}}(o)|^2 \chi^s_{\underline{k}} = \langle |u_{\underline{k}}(o)|^2 \rangle_{E_F} \int \chi^s(E_{\underline{k}}) \rho(E_{\underline{k}}) \, dE_{\underline{k}}$$

Using equation (10'), we can write

$$\chi^s = \sum_{\underline{k}} \chi^s_{\underline{k}} = \int \chi^s_{\underline{k}} \, g(E_{\underline{k}}, A) \, dE_{\underline{k}} \, dA$$

$$= \int \chi^s(E_{\underline{k}}) \, g(E_{\underline{k}}, A) \, dE_{\underline{k}} \, dA$$

or

$$\chi^s = \int \chi^s(E_k)\, \rho(E_k)\, dE_k \tag{19}$$

Combining equations (11), (18), and (19), we get the interaction with the jth nuclear spin to be

$$\mathcal{H}_{1j} = -\gamma\hbar\, I_{zj} \left[\frac{8\pi}{3} \left\langle |u_k(o)|^2 \right\rangle_{E_F} \chi^s \right] H_o \tag{20}$$

This interaction represents an extra magnetic field added to the applied magnetic field H_o which gives rise to the Knight shift. The Knight shift can then be written

$$\frac{\Delta H}{H_o} = \frac{8\pi}{3} \left\langle |u_k(o)|^2 \right\rangle_{E_F} \chi^s \tag{21}$$

If ξ is defined as the ratio $\dfrac{\left\langle |u_k(o)|^2 \right\rangle_{E_F}}{|u_A(o)|^2}$

where $|u_A(o)|^2$ is the probability density of electrons in a free atom, then the expression for the Knight shift can be written in terms of the free atom hyperfine coupling constant.

$$a(s) = \frac{16\pi}{3} \gamma\hbar\, \beta |u_A(o)|^2 \tag{22}$$

Equation (21) then becomes

$$(23) \qquad \frac{\Delta H}{H_o} = \frac{a(s)\,\xi\,\chi_p\,M}{2\gamma\hbar\beta}$$

In order to conform with more usual notation[2], χ^s has been rewritten as $\chi_p M$, where χ_p is the Pauli susceptibility per unit mass and M is the atomic mass.

Equation (23) is the expression for the Knight shift in a crystal with at least cubic symmetry. If the crystal has tetragonal symmetry as does white tin, then equation (23) represents the isotropic part of the Knight shift. As was mentioned earlier, the dipole-dipole interactions in the Hamiltonian of equation (1) will contribute an anisotropic term to the expression for the Knight shift[7].

Consider the Hamiltonian

$$(24) \qquad \mathcal{H}_{anis} = -2\beta\gamma\,\underset{\sim}{I}_j \cdot \left[\frac{\underset{\sim}{S}}{r^3} - \frac{3\underset{\sim}{r}\,(\underset{\sim}{S}\cdot\underset{\sim}{r})}{r^5}\right]$$

If the angle between H_o and the radius vector $\underset{\sim}{r}$ is α, equation (24) becomes

$$(25) \qquad \mathcal{H}_{anis} = \pm\,\gamma\hbar\,m_I\,(1 - 3\cos^2\alpha)\,r^{-3}$$

where the + or - sign is determined by the electron spin being parallel or antiparallel to the magnetic field H_o.

To determine the energy difference due to this Hamiltonian for a nucleus of spin $\frac{1}{2}$ ($\Delta m_I = 1$), we must integrate equation (25) over the electronic wave functions in a way similar to that done for the isotropic case. For a unit volume, only the $2\beta H_o N(E_F)$ electrons with unbalanced spin near the Fermi surface will contribute to the interaction arising from $\mathcal{H}_{anis}$. If V_o is the atomic volume, the energy difference due to $\mathcal{H}_{anis}$ is

$$\Delta W_{anis} = \gamma_N \hbar \beta \cdot 2\beta H_o V_o N(E_F) \left\langle \int \psi^*_{e\underline{k}} \times (3\cos^2\alpha_{\underline{k}} - 1) |r_k|^{-3} \psi_{e\underline{k}} \, dV \right\rangle_{E_F} \tag{26}$$

where $\psi_{e\underline{k}}$ is the electronic wave function of an electron in the $\underline{k}$ th state. If we introduce an average wave function ψ so that $\psi\psi^*$ represents the average electron density in space of the conduction electrons near the Fermi surface, then equation (26) gives for the anisotropic part of the Knight shift

$$\frac{\Delta H_{anis}}{H_o} = 2\beta^2 V_o N(E_F) \int \psi^* (3\cos^2\alpha - 1) |r|^{-3} \psi \, dxdydz \tag{27}$$

To evaluate this integral, we let the field have the polar angles Θ and Φ and the radius vector $\underline{r}$ have polar

angles Θ and Φ with respect to the x, y, z coordinate system. The term $(1 - 3\cos^2\alpha)$ can then be expressed in terms of these angles by a well known addition theorem in terms of tesseral harmonics in the angles θ and φ and Θ and Φ respectively

$$(28)\quad \tfrac{1}{2}(3\cos^2\alpha - 1) = \sum_{m=-2}^{2} (-1)^m P_2^m(\cos\Theta)\, P_2^{-m}(\cos\theta) \times e^{im(\Phi - \Theta)}$$

We assume that Ψ can be represented by a mixture of p-wave functions of the form Ψ_o, $\frac{1}{\sqrt{2}}(\Psi_+ + \Psi_-)$ and $\frac{1}{\sqrt{2}}(\Psi_+ - \Psi_-)$. These wave functions are real and therefore represent quenched p orbitals. For axial symmetry, the electron density can be written as

$$(29)\quad \Psi\Psi^* = g(r)\left[A(x^2 + y^2) + Cz^2\right] = r^2 g(r)\left[A + (C - A) \times \cos^2\Theta\right]$$

where $g(r)$ is a radial distribution function whose form is unimportant for this calculation. Substituting equations (29) and (28) into equation (27), we get

$$(30)\quad \frac{\Delta H_{anis}}{H_o} = \beta^2 V_o N(E_F) q(3\cos^2\theta - 1)$$

where θ is the angle between the z axis and the applied magnetic field, and q is given by

$$q = \int \psi^* (3\cos^2\theta - 1)\,|r|^{-3}\,\psi\, dV$$

$$= \frac{16\pi}{5}(C - A)\int_0^\infty r\, g(r)\, dr$$

q is the electric field gradient at the nucleus caused by electrons near the Fermi surface.

In order to explore the orientation dependence of the Knight shift with respect to the magnetic field, we can rewrite this expression as

$$\frac{\Delta H_{anis}}{H_o} = \text{constant} \cdot (3\cos^2\theta - 1) \tag{31}$$

The total Knight shift including the anisotropic part is then given by equations (23) and (31) and can be written[8]

$$\frac{\Delta H}{H_o} = K + \tfrac{1}{2} K'_{\parallel}\,(3\cos^2\theta - 1) \tag{32}$$

CHAPTER 3

EXPERIMENTAL APPARATUS AND TECHNIQUE

The nuclear magnetic resonance spectrometer used in this work is essentially of standard design. Figure 1 is a schematic diagram of the spectrometer. The circuit diagrams are all given in Appendix C.

Since the object of the experiments has been to measure resonance frequencies and line shapes, a Pound-Knight-Watkins[9] marginal oscillator was chosen for this work. The oscillator was very slightly modified from the original design. Instead of a 6J6 tube, a 396A was used as the oscillator tube. Also the rf amplifier was fed from the cathodes of the 396A instead of from the grid to which the sample coil was attached. The capacitance for the resonant circuit was provided by a Varicap (variable capacity diode). The frequency of the oscillator was then swept by varying the voltage across the diode. The voltage source for the diode was provided by the sawtooth waveform from a modified Tektronix waveform generator[10,11]. The modified waveform generator can provide a negative going sawtooth voltage from 100 to 0 volts with periods which vary from several seconds to several hours.

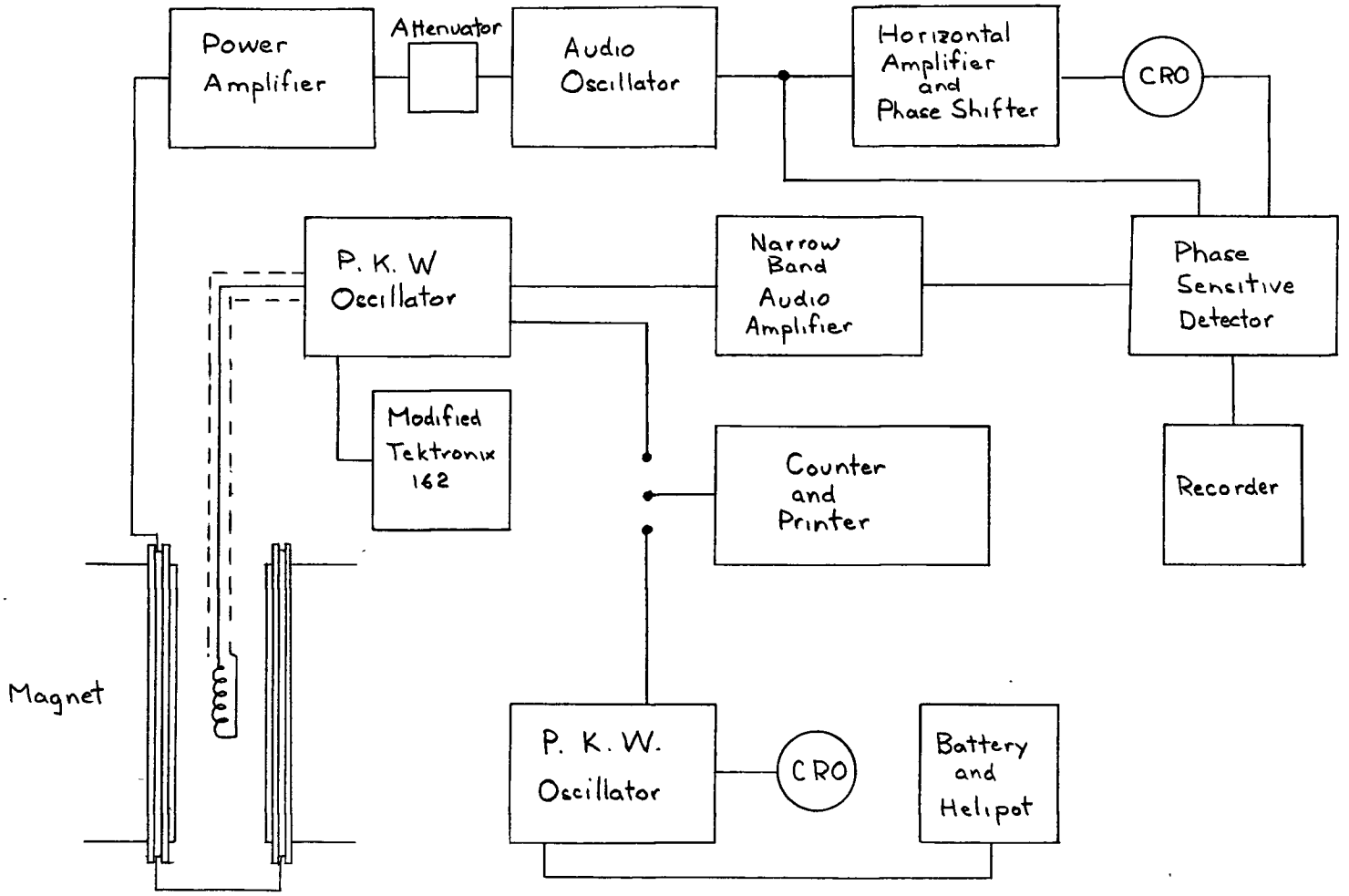

Figure 1. Block Diagram of the Spectrometer

Any voltage between 10 and 100 volts can be used as the initial voltage of the sawtooth and the sawtooth rundown can be stopped at any time with the voltage returning to its initial set value. Using a Varicap instead of a variable air condenser eliminates noise from a driving motor and provides a more uniform frequency sweep, especially at the slower rates.

Following the marginal oscillator is a model 216 White twin tee narrow band audio amplifier. Two bandwidths at 15 cps were used in this work: a 23% bandwidth (about 4 cps) network and a 1.3% (about .2 cps) network. The latter bandwidth corresponds to a time constant of about 5 seconds and thus was used only for comparatively slow frequency sweeps.

The phase sensitive detector used is in principle the same as Shuster's[12], although different tubes were employed. The signal recorder was a Varian recorder, model G11A.

The frequency of the oscillator as it swept through the signal was monitored by a Hewlett-Packard electronic counter, model 524C, with the appropriate plug-in unit. The frequency measured was in all cases the average frequency over .1 second. The frequency reading was recorded by a Hewlett-Packard digital recorder, model 516B. The digital recorder in turn activated an indicator pen on the signal recorder each time the electronic counter measured the frequency. This method of measuring and recording frequency gave fast, accurate, and frequent monitoring of the oscillator frequency as it

passed through the nuclear magnetic resonance signal.

The magnet used throughout this work was a Varian rotating magnet with twelve inch pole faces and a 2 1/4 inch gap and was capable of giving a magnetic field of 11.4 kilogauss. Modulation of the magnetic field was accomplished using two modulation coils each wound with 60 turns of No. 18 copper wire on bakelite forms which were mounted around the pole caps. The modulation coils were supplied by an audio oscillator through a 20 watt power amplifier.

A schematic diagram of the low temperature system is given in Figure 2. The helium cryostat is a standard double glass dewar system. Temperatures down to 1.15°K were obtained by pumping on the liquid helium with a 3 inch Kinney pump. The temperature was controlled by controlling the pumping speed with a needle valve in parallel with a $1\frac{1}{2}$ inch vacuum valve, and was measured by observing the vapour pressure of the helium with a mercury manometer in parallel with one containing di-butylpthalate. The dewars and dewar cap were mounted so that they could slide in and out from between the magnet pole faces.

The sample was mounted on the end of a 3/8 inch thin wall stainless steel tube which formed the outer conductor of the coaxial line connecting the sample coil to the marginal oscillator. The centre conductor of the coaxial line was a No. 32 copper wire held in place with teflon spacers.

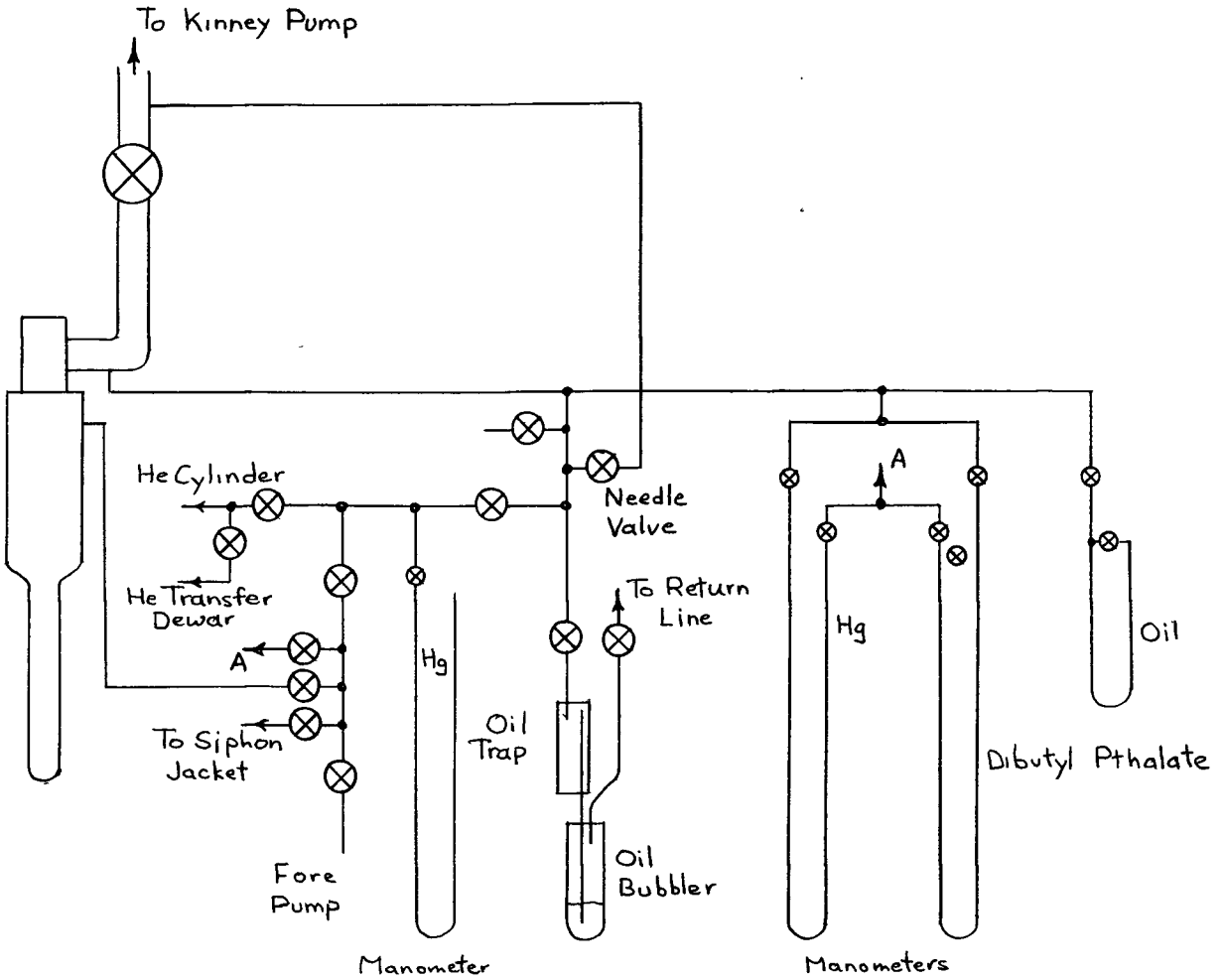

Figure 2. Schematic Diagram of the Low Temperature System

Three semi-circular radiation shields made from sheet metal copper were mounted on the stainless steel coaxial line.

The tin single crystal was made from "Extra Pure" tin, VS-151, obtained from the Vulcan Detinning Company. The purity quoted was 99.999+% tin with impurities of .0008% lead and .000018% iron. The single crystal was grown by pouring molten tin into a $\frac{1}{2}$ inch by $\frac{1}{2}$ inch by 4 inch graphite mold, then slowly (one inch every 14 minutes) withdrawing the mold from the furnace. In order to grow a crystal with the desired orientation, that is with the [001] direction approximately perpendicular to the crystal axis, a seed crystal which had the desired orientation was used. The seed was joined to the molten tin just outside the furnace mouth by drawing out a small stream of tin from the main melt with a glass rod. The interface of the seed and molten tin was "puddled" or stirred until the seed began to melt back from the interface. The mold was then withdrawn from the furnace as described above. The cast tin slab thus obtained was etched electrolytically in a fairly dilute HCl solution, and if no grain boundaries were apparent, an X-ray photograph was taken (Laue back reflection photograph) to determine the crystal orientation. This method will give the orientation to within about one degree.

The seeds were prepared and analysed in a similar manner. Instead of drawing the molten tin out to join a seed

as described above, it was drawn out to a fine point. The first tip of this point to solidify does so to form a single crystal which is then propagated along the whole specimen as it is withdrawn from the furnace. By using this seed placed properly in the mold, a new seed with an orientation closer to the desired orientation can be grown. This process is continued until a suitable seed crystal is obtained which is then used for all subsequent crystals.

Once a crystal quite near the desired orientation was obtained, it was sliced along planes containing the [001] axis with a jeweller's saw into slices about 1 mm thick. These slices were etched in a mixture of concentrated HCl and HNO_3 for a few minutes until they were about .3 mm thick. They were then glued together with Q dope. The resulting laminated crystal was made up of thirty slices and was about $\frac{1}{2}$ inch by $\frac{1}{2}$ inch by 3/8 inch.

The crystal slices were aligned probably to within one degree and possibly better. The error of alignment would seem then to be of the same order of magnitude as the error in determining the crystal orientation from the X-ray photograph. Although no subgrain boundaries were observed, they may well have been present and could give a misalignment of perhaps one-half degree. The experiments performed were mostly not sensitive to misalignments of less than a few degrees, and no evidence of misalignment was observed.

The aluminum crystal was obtained commercially from Metals Research Ltd., Cambridge. It was a cylindrical specimen $\frac{1}{2}$ inch diameter by 3/4 inch long and was made from 99.9999% pure aluminum.

For experiments with both the aluminum and tin crystals, the sample coil was wound directly on the crystal rather than having the coil and crystal separated by a layer of some insulator like electrical tape or mylar. In order to have the oscillator oscillate at the correct frequency with minimum capacity, a four strand $4\frac{1}{2}$ turn coil wound from No. 28 wire was used on the tin crystal and a fifty turn coil of No. 28 wire was wound around the aluminum crystal. Winding the coil directly on the aluminum crystal improved the signal-to-noise ratio considerably, presumably because the filling factor of the coil was increased and because the inductance of the coil was reduced, allowing the coil to have a greater number of turns. Using No. 32 wire further reduced the inductance, but with more than about 40 turns in the coil, the low Q of the inductance prevented the oscillator from oscillating.

Because the magnetic field drifts somewhat during an experiment, the procedure followed was to measure the magnetic field frequently with a probe containing D_2O mounted just outside the dewars. The deuteron resonance was observed directly on an oscilloscope through a wide band audio amplifier while at the same time the oscillator frequency was

measured with the Hewlett Packard frequency meter. For the measurements of the anisotropic Knight shift, the magnetic field was measured before and after each set of readings taken at a particular crystal orientation. The second field measurement often agreed with the first to within one part in 600,000 and never differed by more than five parts in 10^6 for the measurement of the tin resonance to be considered valid. For the measurements described in Chapter 5, somewhat more care was taken in measuring the field. The field was measured before and after every metal resonance and did not differ by more than two parts in 600,000 for the measurement to be considered valid.

Almost all of the resonances were recorded using 5 or 10 second time constants in the phase sensitive detector. Nearly all of the tin resonances were observed using a modulation of less than one-third gauss. For the aluminum resonances where there seemed to be some problems of saturation and where only the resonance frequency was wanted, the modulation used was increased from less than two gauss to about four gauss for the last set of measurements. Figures 3 and 4 show typical tin and aluminum signals at 1.15° K.

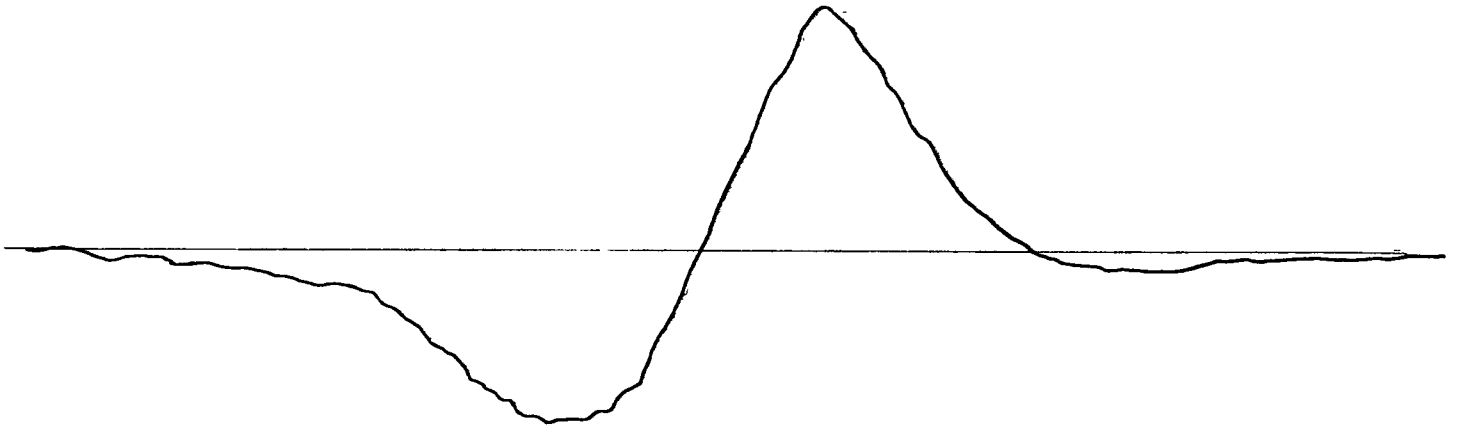

Figure 4. Derivative of the Al Resonance

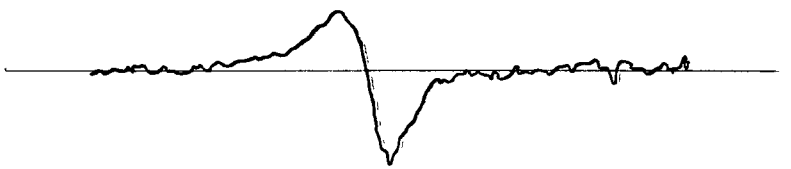

Figure 3. Derivative of the Sn Resonance

CHAPTER 4

THE KNIGHT SHIFT AND LINE WIDTH OF THE TIN SINGLE CRYSTAL

Measurements of the nuclear magnetic resonance of Sn^{117} and Sn^{119} in the single crystal of white tin described in Chapter 3 were made as a function of the crystal orientation in the applied magnetic field, as a function of the applied magnetic field, and as a function of temperature in the liquid helium range. Figure 5 summarizes some of these results. The different curves show the variation of the Knight shift as the external field is rotated through an angle of 180° at temperatures of 4.2°K and 1.15°K and at fields of 10.1 kilogauss and 6.13 kilogauss. The Knight shift was found to be equal within experimental errors for both isotopes. Measurements of the Knight shift as a function of crystal orientation in two different planes of rotation[13] (appendix B) assured that the electronic environment of the nucleus showed tetragonal symmetry. All of the measurements recorded in this chapter were made in the crystal plane containing the [001] axis. Table 1 gives values of K and $K'_{\parallel}$ for different temperatures and applied magnetic fields.

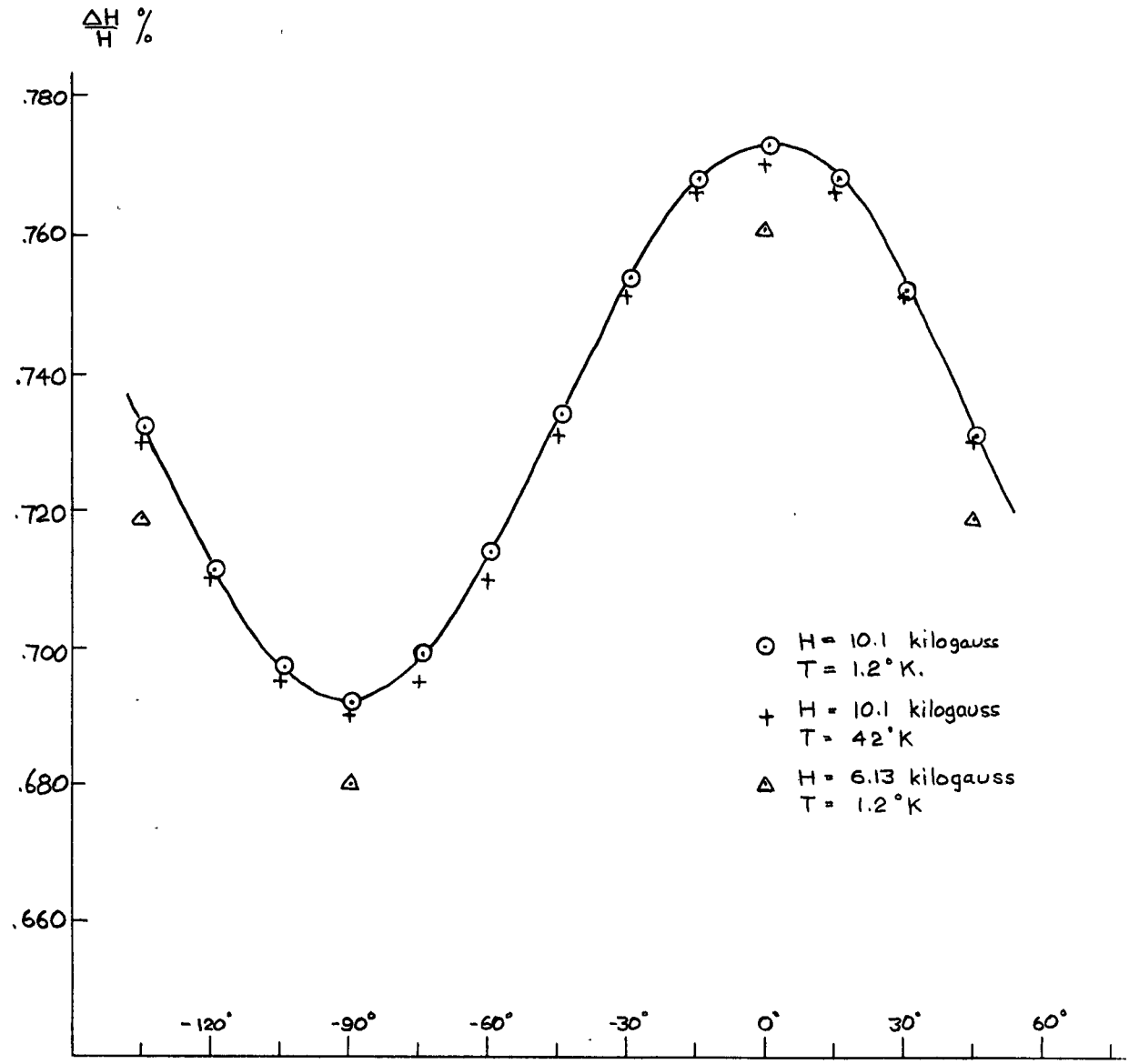

Fig. 5. The Knight Shift in Tin as a Function of the Crystal Orientation in the Magnetic Field (Orientation measured from the [001] axis)

TABLE 1

Temperature	Field	$K \times 10^4$	$K'_{\parallel} \times 10^4$
1.15° K	10.1 kg	$71.9 \pm .1$	$5.4 \pm .1$
4.2° K	10.1 kg	$71.6 \pm .1$	$5.4 \pm .1$
1.15° K	6.13 kg	$70.7 \pm .2$	$5.4 \pm .2$

As has been noted by Bloembergen and Rowland[7], $K'_{\parallel}$ is positive indicating that q of equation (30) is positive. Furthermore, $K'_{\parallel}$ is quite large, almost ten percent of K. Because the hyperfine interaction for p-wave functions is less than for s-wave functions and because only the anisotropic part of the p-wave function interaction contributes to $K'_{\parallel}$, the large value of $K'_{\parallel}$ indicates a substantial p-wave function component in the electronic wave function.

In metals whose specimen size is large compared to their skin depth, the power absorbed by the sample is proportional to $\chi' + \chi''$, the real and imaginary parts of the nuclear spin susceptibility, rather than to χ'' alone as would be the case for non-metals or for metals whose particle size is small compared to their skin depth. Chapman, Rhodes, and Seymour[14] have determined that this effect would decrease the

measured zero of the derivative of the observed absorption signal by about .3 of the line width as determined from the maxima of the derivative. This would decrease K by about $.2 \times 10^{-4}$ or less than one-half percent of the value of K. It would also decrease the value of $K'_{\parallel}$ by about one percent of its value. The corrections to K and $K'_{\parallel}$ may well be even smaller because, as noted by Karimov and Shchegolev[15], for resonant circuits of low Q as is the case when the coil of the circuit is wound on a metal specimen, the contribution of χ' to the observed absorption may be quite small. That this could be true in our case is substantiated by the large degree of symmetry shown by the observed absorption curve. Figure 6 shows the asymmetry expected in the derivative of Lorentzian and Gaussian line shapes. The ratio of the amplitudes of the extrema of the derivative of the Lorentzian curve is .39 and of the Gaussian curve is .55, but the ratio of the observed derivative was about .7. This means either the line shape of the observed resonance is "squarer" than a Gaussian line shape or that the dispersion mode does not contribute equally with the absorption mode to the observed resonance. Since the corrections to K and $K'_{\parallel}$ computed on the basis of equal contributions from both the absorption and dispersion modes are just barely larger than the errors in the measured K and $K'_{\parallel}$, when the additional point of unequal contributions is considered it seems unnecessary to make any corrections to

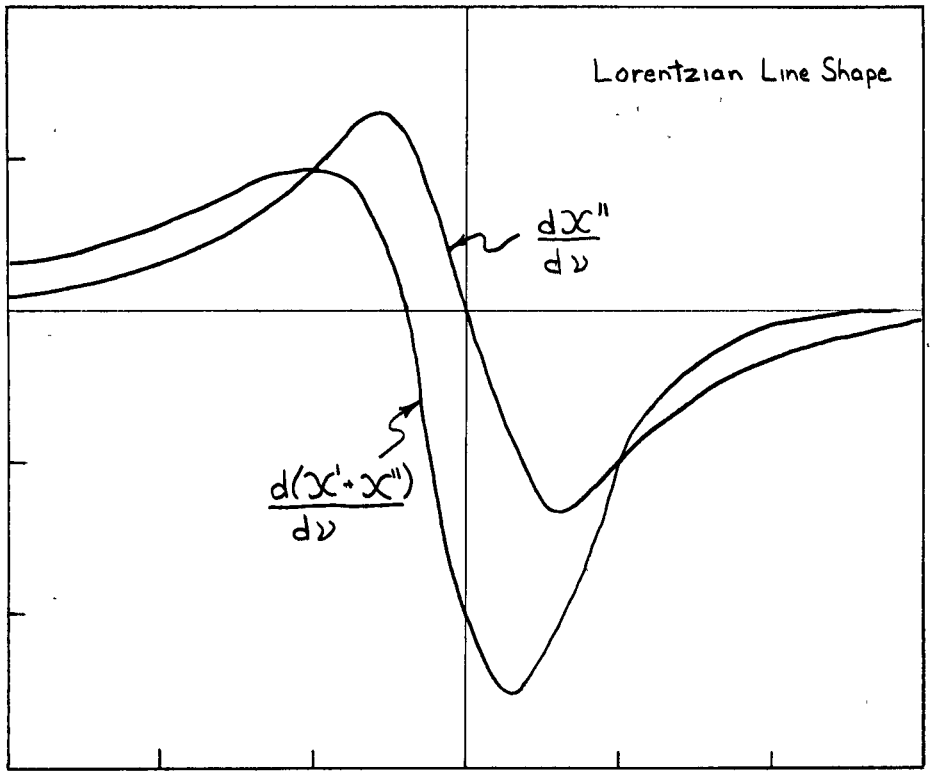
Lorentzian Line Shape
$\frac{d\chi''}{d\nu}$
$\frac{d(\chi'+\chi'')}{d\nu}$

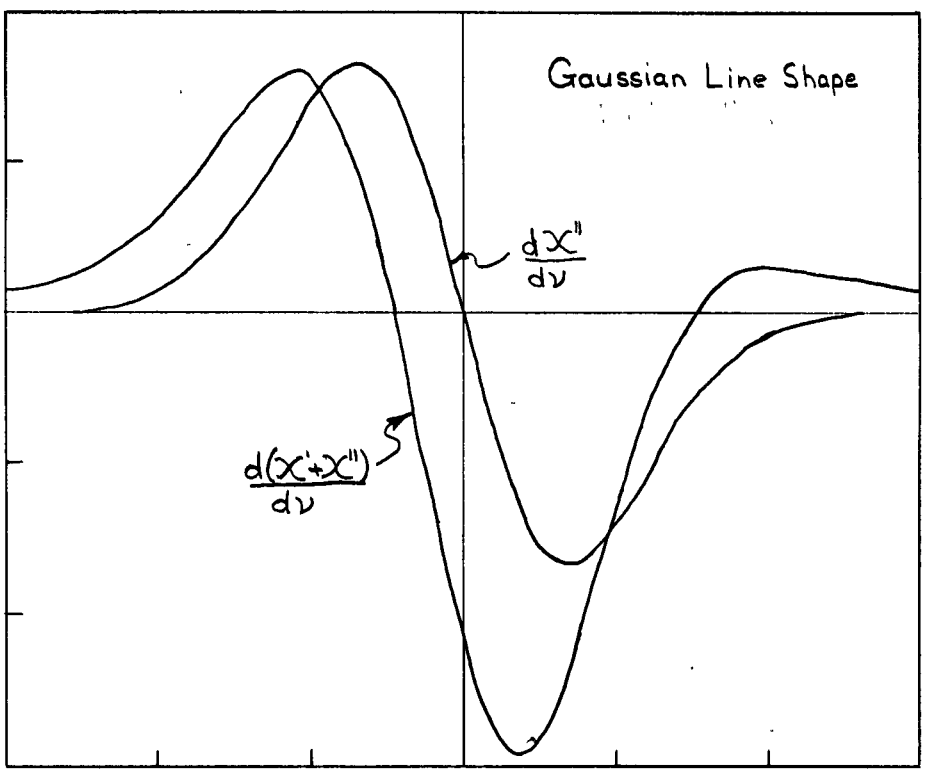
Gaussian Line Shape
$\frac{d\chi''}{d\nu}$
$\frac{d(\chi'+\chi'')}{d\nu}$

Figure 6.

the observed results.

Figure 7 shows the line width of the tin specimen as determined by the extrema in the derivatives of absorption lines. The line width cannot be explained in terms of dipole-dipole coupling between nearest neighbours alone. The second moment, $\overline{\Delta\omega^2}$, for dipole-dipole coupling for a substance with two spins is given by Van Vleck[16]

$$\overline{\Delta\omega_I^2} = \overline{(\Delta\omega_I^2)_{II}} + \overline{(\Delta\omega_I^2)_{IS}} \tag{33}$$

where

$$\overline{(\Delta\omega_I^2)_{II}} = \frac{3}{4}\gamma_I^4 \hbar^2 I(I+1) \sum_k \frac{(1 - 3\cos^2\theta_{jk})^2}{r_{jk}^6}$$

and

$$\overline{(\Delta\omega_I^2)_{IS}} = \frac{1}{3}\gamma_I^2 \gamma_S^2 S(S+1) \hbar^2 \sum_k \frac{(1 - 3\cos^2\theta_{jk})^2}{r_{jk}^6}$$

are the contributions to a nucleus from like nuclei labelled I and unlike nuclei labelled S. In the case of tin, for $\theta_{jk} = 0$ only the two nearest neighbours give a significant contribution to the second moment. When the natural abundances of the two tin isotopes are considered, this formula

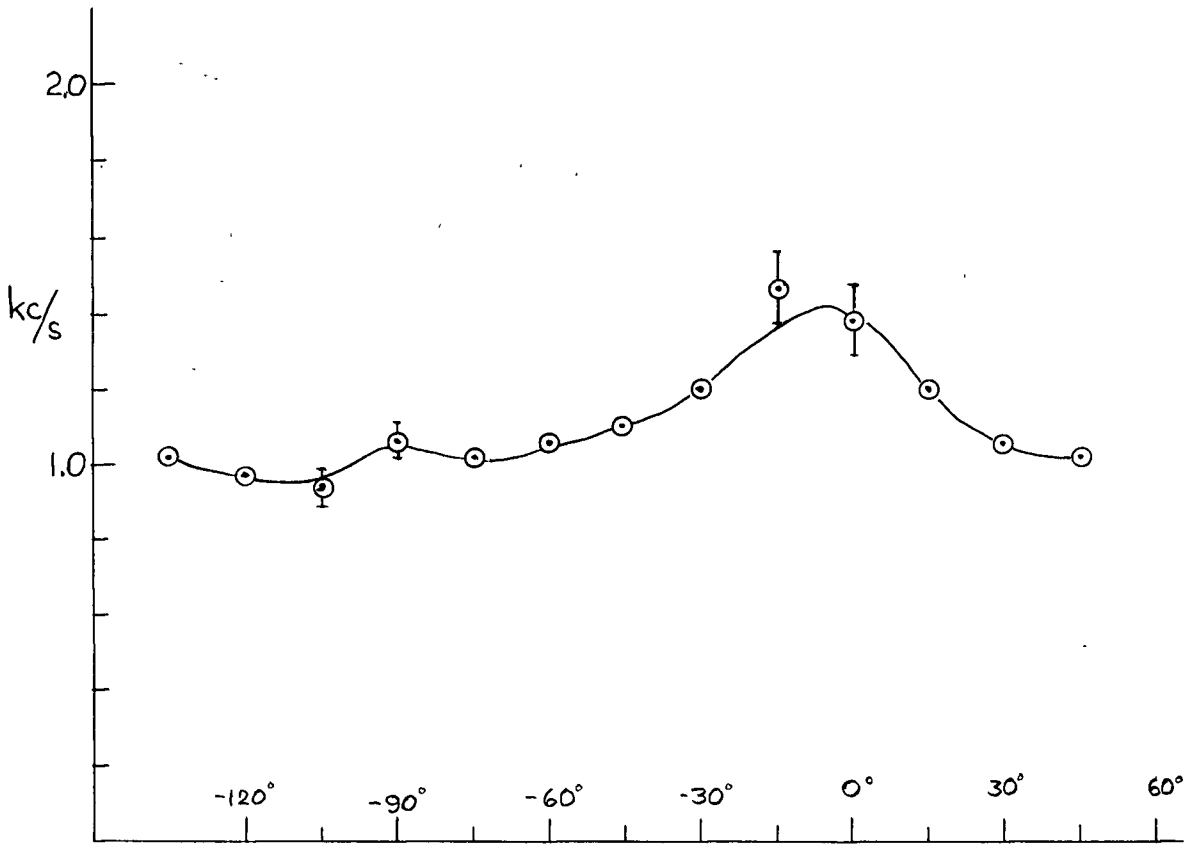

Figure 7. The Line Width of the Tin Resonance as a Function of the Crystal Orientation in the Magnetic Field
(Orientation measured from the [001] axis)

gives a second moment of .15 $(kc/s)^2$ at $\theta_{jk} = 0$. Taking the second moment of the observed signal to be approximately equal to the square of the separation of the extrema of the derivative of the resonance signal, we get a result of 2 $(kc/s)^2$, more than ten times the theoretical value. If the line shape is in fact Gaussian, the experimental second moment is 1.6 $(kc/s)^2$.

If the calculated second moment due to dipole-dipole interactions is subtracted from the observed second moment, there remains an isotropic second moment of .6 $(kc/s)^2$. One possible origin of this second moment is broadening due to misalignment of the slices which make up the crystal specimen (although this broadening will not be isotropic). A simple calculation (see Appendix A) shows this second moment to be

$$(34) \qquad \overline{(\nu-\bar{\nu})^2} = \left(\frac{\Delta\nu_{\parallel}'}{2}\right)^2 \left\{ 12 \cos^2\theta \cos^2\alpha \sin^2\theta \sin^2\alpha + \frac{4}{5} \sin^4\theta \sin^4\alpha \right\}$$

where $\Delta\nu_{\parallel}' = K_{\parallel}' \gamma H_o$, θ is the angle between the [001] crystal axis and the magnetic field, and α is a parameter expressing the degree of misalignment. The contribution to the second moment will be greatest for $\theta = 45°$. Misalignment is believed to be the explanation for previously reported broad lines[13]. In order to explain the measured second

moment of .6 $(kc/s)^2$, α must be set at 18°, an improbably high figure. Further, a study of the line width as a function of magnetic field for $\Theta = 45°$ revealed no change in the line width when the field went from 10.1 kilogauss to 6.13 kilogauss. The uncertainty in the measurement of the line width was about .1 kc/s. Assuming the change in line width over this region of magnetic field to be the maximum value within this uncertainty, we find the corresponding change in the second moment would mean a misalignment of $\alpha = 4°$, still a somewhat high value.

If it is assumed that misalignment of the crystal slices (or misalignment due to sub grain boundaries) does not contribute to the line width, then there must be some fairly large isotropic broadening mechanism such as that arising from indirect exchange interactions[17,18] between the two tin isotopes which contributes to the line width. Karimov and Shchegolev[15] suggested that this mechanism is present in tin and attributed a second moment of about .5 $(kc/s)^2$ to it.

Indirect exchange interactions in metals result from a coupling between the magnetic moments of two nuclei by way of their conduction electrons and the hyperfine interaction. If only the contact term of the spin Hamiltonian of equation (1) is considered, this coupling is purely scalar[19]. The exchange interaction energy between unlike nuclear spins in a metal is of the form[17]

$$(35) \qquad \mathcal{H} = \sum_{i>j} \sum_{j} A_{ij} \underline{I}_i \cdot \underline{I}_j$$

Van Vleck[16] shows that the second moment of the absorption line of the nuclei with one magnetic moment due to the exchange interaction with the nuclei of another magnetic moment is

$$(36) \qquad h^2 \overline{(\Delta\nu)^2} = \frac{1}{3} I(I+1) f \sum_{j} A_{ij}^2$$

where f is the fraction of the lattice sites occupied by the nuclei with the different magnetic moment. He also shows in the same paper that exchange interactions between nuclei of like magnetic moments do not contribute to the second moment of the resonance line.

Several assumptions are made to calculate A_{ij}. It is assumed that the energy $E_{\underline{k}}$ is given by $E_k = \frac{\hbar^2 k^2}{2m^*}$, where m* is the effective mass of the electrons with wave number k. The number of orbital states $Z(\underline{k})\, d^3k$ in the space of wave vectors is assumed to be $\frac{V d^3k}{(2\pi)^3}$, the number for free electrons. Also the excited states E_k, are assumed to extend from the Fermi level, $E_F = \frac{\hbar^2 k_F}{2m^*}$, to infinity, that is, there are no energy gaps just above the Fermi surface. Finally, it is assumed that the main contribution to the exchange interaction comes from values of $\underline{k}$ such that $|\underline{k}^2 - \underline{k}'|^2$ is very small, and that $|\underline{k}| \approx |\underline{k}'| \approx |k_F|$,

$\underline{k}$ being the wave vector of a filled state and $\underline{k}'$ of an unfilled state. Under these assumptions, the scalar coupling coefficient becomes

$$(37) \quad A_{ij} = \frac{\Omega^2 \, m^* \xi \, \nu_a \, (i) \, \xi \, \nu_a(j)}{2\pi (2I_i + 1)(2I_j + 1)} \left(\frac{1}{R_{ij}}\right)^4 \left\{ 2k_F \, R_{ij} \cos(2k_F R_{ij}) - \sin 2k_F R_{ij} \right\}$$

where Ω is the atomic volume

m^* is the effective mass of the electron involved in the exchange interaction

ξ is the ratio of the hyperfine interaction in crystal to that in a free atom

ν_a is the observed atomic hyperfine structure splitting

R_{ij} is the separation of the two nuclear spins I_i and I_j

k_F is the wave vector of an electron at the Fermi surface

It is difficult to ascribe a value to A_{ij} for tin given by this formula because tin does not have even a nearly spherical Fermi surface. However, assuming that this formula for A_{ij} is not entirely invalid, we can make an order of magnitude estimation of the second moment due to exchange

broadening. It is assumed that $m = m^*$. This is not true for all electrons as is shown by the many periods of the de Haas-van Alphen oscillations in tin[20,22] which give values of $\frac{m^*}{m}$ varying between .05 and 1.0. From electronic specific heat measurements, $\frac{m^*}{m}$ is found to be 1.2. Likewise the value of the wave vector k_F depends on which part of the Fermi surface is being considered, but some average value can be approximated using the measured values of the electronic specific heat. Within the limits of these approximations, it is reasonable to assume $\xi = 1$, and to assume some average value of ν_a measured in the different fine structure levels of the ground state of the free atom of tin[21].

In order to perform the summation of equation (36), we perform the sum over the first n-1 shells of nearest neighbours, and replace the sum by an integral for the rest.

$$(38)\qquad \sum_j A_{ij}^2 = A^2 \sum_{j=1}^{n-1} \left(\frac{1}{R_{ij}}\right)^8 \Big\{ 4k_F^2 R_{ij}^2 \cos^2(2k_F R_{ij}) + \sin^2(2k_F R_{ij}) - 4k_F R_{ij} \cos(2k_F R_{ij}) \sin(2k_F R_{ij}) \Big\}$$
$$+ A^2 \Big\{ \rho \int_{Rin}^{\infty} \frac{4k_F^2 R_{ij}^2 \cos^2(2k_F R_{ij})}{R_{ij}^8}\, dV$$
$$+ \rho \int_{Rin}^{\infty} \frac{\sin^2(2k_F R_{ij})}{R_{ij}^8}\, dV$$
$$- \rho \int_{Rin}^{\infty} \frac{4k_F R_{ij} \cos(2k_F R_{ij}) \sin(2k_F R_{ij})}{R_{ij}^8}\, dV$$

where A represents the constant terms in equation (37), $dV = 4\pi R_{ij}^2\, dR_{ij}$, and ρ is the number of atoms per unit volume. The three integral terms give

$$(39)\quad \sum_{j=n}^{\infty} A_{ij}^2 = 4\pi\rho\,(2k_F)^5\,A^2 \left\{ \frac{\cos^2 a}{3a^3} + \frac{\sin^2 a}{5a^2} + \sin b \times \left\{ -\frac{2}{15b^2} - \frac{16}{5b^4} \right\} + \cos b \left\{ -\frac{2}{15b} - \frac{16}{15b^3} \right\} + \text{si } b \left\{ \frac{2}{15} \right\} \right\}$$

where

$$\text{si } b = -\int_b^{\infty} \frac{\sin x}{x}\, dx$$

and

$$b = 2a = 4k_F\, Rin$$

For large b (in our case $b \approx 80$), si b can be expanded in a series, and the sum can be written

$$(40)\quad \sum_{j-n} A_{ij}^2 = 4\pi\rho A^2 (2k_F)^5 \left\{ \frac{\cos^2 a}{3a^3} - \frac{4}{3}\frac{\cos b}{b^3} - \frac{4\sin b}{b^4} + \frac{\sin^2 a}{5a^5} + \frac{16\cos b}{5b^5} + O\left(\frac{1}{b^6}\right) \right\}$$

Using an IBM 1620 computer, equation (38) was evaluated for k_F between .5 x 10^8 cm^{-1} and 2.5 x 10^8 cm^{-1} at intervals of .01 by performing the sum over fifteen shells (84 nearest neighbours) and replacing the sum by an integral from the sixteenth shell outwards. Figure 8 shows the result of this calculation with a plot of $\sum_j \frac{A_{ij}^2}{A^2}$ vs k_F. As can be seen, the sum is very sensitive to k_F. The value of k_F obtained from the electronic specific heat of tin is 1.5 x 10^8 cm^{-1}, which happens to be near a maximum point of the curve. Thus a small error in k_F, although it will cause a considerable error in $\sum_j \frac{A_{ij}^2}{A^2}$, will give less error than another value might. Further, this value of k_F will give the upper limit to the exchange broadening coefficient unless the correct value of k_F is considerably larger than that expected from electronic specific heat measurements. For $k_F = 1.5 \times 10^8$ cm^{-1}, $\sum_j \frac{A_{ij}^2}{A^2} = 1.75 \times 10^{62}$. The integral part of equation (38) contributes only about one percent to this sum, and the terms neglected, those of the order $4\pi\rho\,(2k_F)^5 \left\{ O\left(\frac{1}{b}\right)^6 \right\}$ are down by a factor of 10^8. In fact, for this value of k_F, the most significant contribution comes from only the first two nearest neighbours in the first shell.

Assuming ν_a to be 10^{10} c/s, we get $A = 2.66 \times 10^{-54}$ and using equation (36), we get $\overline{(\Delta\nu)^2} = .57$ $(kc/s)^2$. This excellent agreement between theory and experiment can be no

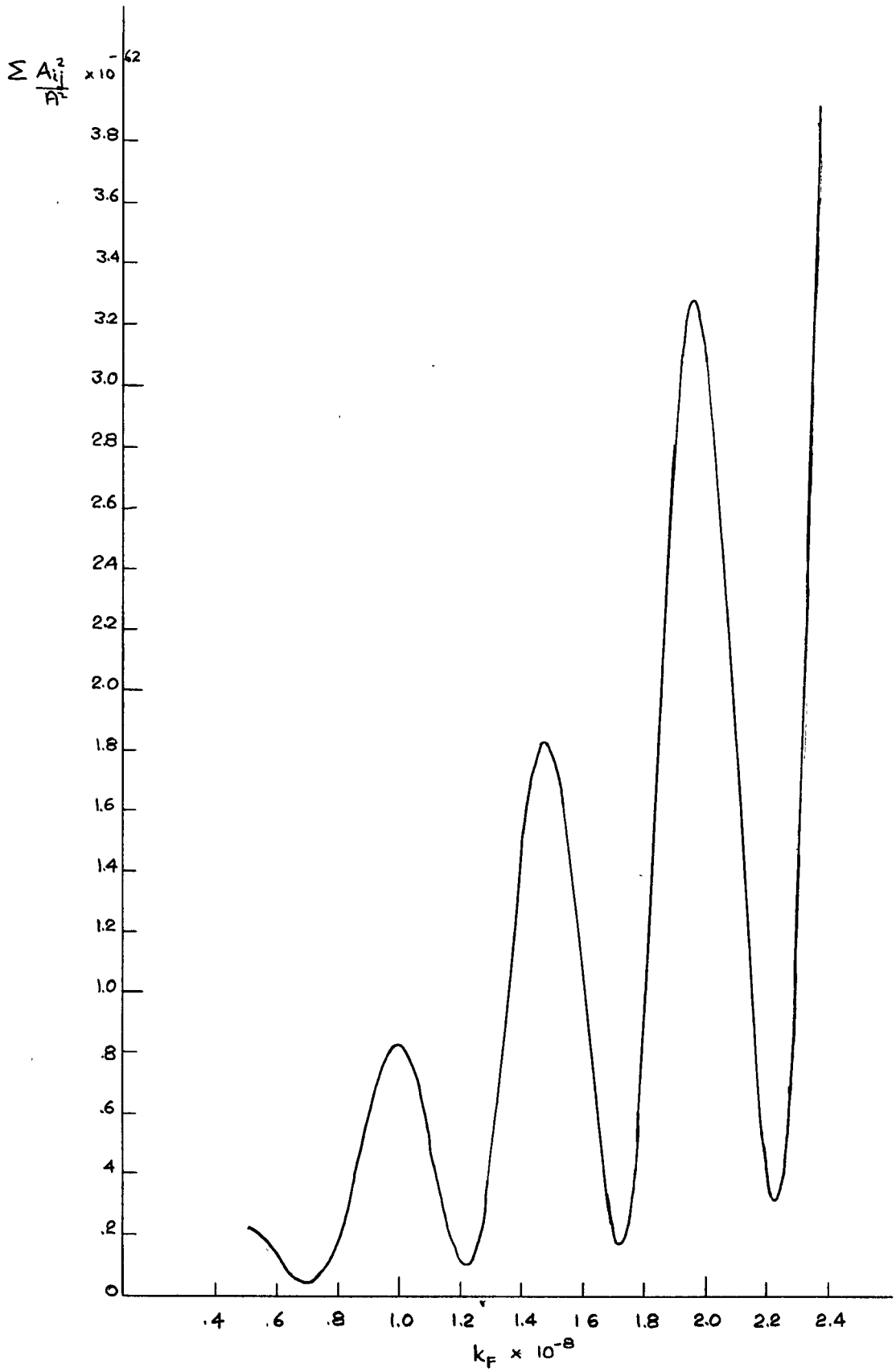
$\Sigma \frac{A_{ij}^2}{P^2}$ x 10^{-62}
3.8
3.6
3.4
3.2
3.0
2.8
2.6
2.4
2.2
2.0
1.8
1.6
1.4
1.2
1.0
.8
.6
.4
.2
0
.4
.6
.8
1.0
1.2
1.4
1.6
1.8
2.0
2.2
2.4
k_F x 10^{-8}

Figure 8.

more than fortuitous considering the approximations involved in deriving the formula for A_{ij}, let alone considering the approximations in the value of the constants such as ν_a and ξ. However, the agreement is encouraging insofar as it gives some justification for choosing k_F in non-cubic metals from measurements of the electronic specific heat and indicates that the approximation of a spherical Fermi surface in the derivation of the expression for A_{ij} may not be particularly restrictive. Because this result can be considered only an order of magnitude calculation, no attempt to separate the quantities χ_p and ξ has been made[2].

Figures 5 and 9 show the temperature dependence of the Sn^{117} and Sn^{119} resonance. The measured change of $\frac{\Delta H}{H}$ in going from 4.2°K to 1.15°K was only - .002% or considerably less than 1% of the total Knight shift. If a free electron model holds, $\frac{\Delta H}{H}$ is expected to vary as $V_o^{-1/3}$, where V_o is the atomic volume[2]. The accuracy of the temperature dependence measurements is too poor over this range of temperature to enable any statement about temperature variation of the Knight shift other than it increases slightly as the temperature is decreased. Figure 5 shows that only K and not $K'_{\parallel}$ is temperature dependent within the accuracy of the experiment.

The magnetic field dependence of the Sn^{117} and Sn^{119} resonances shown in Figures 5 and 10 is fairly small over the range of fields considered, but is well outside

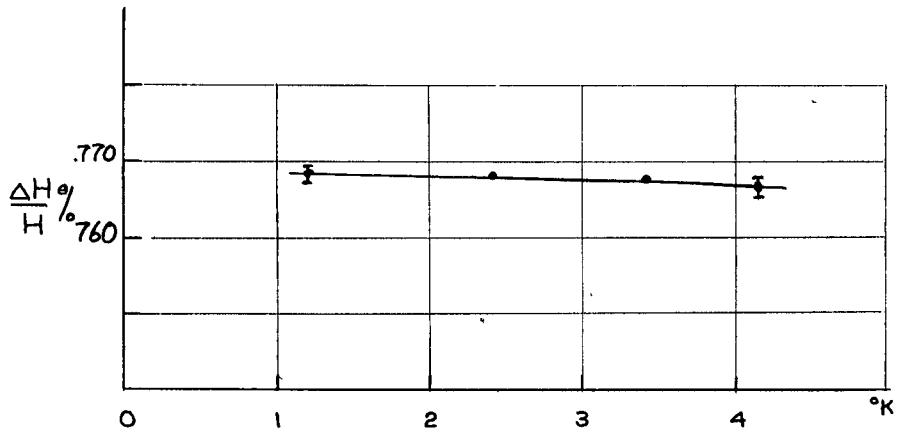

Figure 9. The Knight Shift in Tin as a function of Temperature

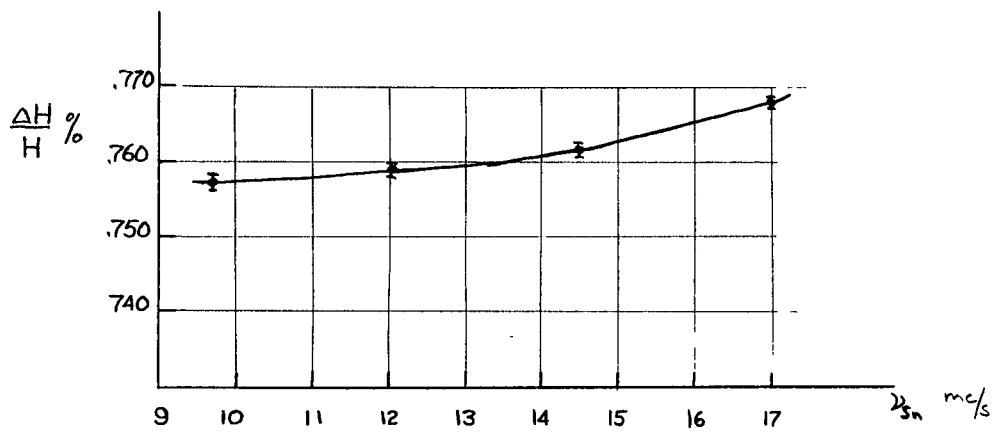

Figure 10. The Knight Shift in Tin as a Function of Magnetic Field (Magnetic field measured in terms of the non-metal Sn resonance)

experimental error. No simple explanation of the field dependence seems to exist since χ_p is believed to be field independent. The field dependence can be explained perhaps in terms of polarization of the ion cores, or in terms of some diamagnetic field dependence.

CHAPTER 5

THE POSSIBILITIES OF DE HAAS-VAN ALPHEN TYPE OSCILLATIONS IN THE KNIGHT SHIFT

As mentioned in Chapters 1 and 2, if the orbital angular momentum of the electrons in a metal is not completely quenched, there exists the possibility of an oscillatory behaviour of the Knight shift caused by oscillations in the diamagnetic susceptibility as the external field is varied. This effect would be similar to the de Haas-van Alphen effect[22,23,24] which has yielded so much information about the Fermi surface of many metals. The idea for this experiment first arose in discussions in this laboratory between Dr. R. Barrie and Dr. M. Bloom who mentioned it to T. P. Das. The problem of calculating the diamagnetic field at the nucleus is rather formidable, although attempts at it have been made by Das and Sondheimer[25] followed by other authors[26,27,28,29,30] and estimates of the change in the Knight shift have been made.

The de Haas-van Alphen effect is a low temperature, high magnetic field phenomenon. Typically, experiments are done at 1.2°K in magnetic fields between 15 and 100 kilogauss.

Although the temperatures required are readily accessible, these magnetic fields are somewhat high for typical nuclear magnetic resonance studies. To obtain fields of 100 kilogauss, Shoenberg[22] and others have used pulsed magnets whose rate of change of field is something like 5×10^6 gauss/sec, quite unsuitable for nuclear magnetic resonance work. The work described here was performed in a field of about 10 kilogauss at 1.15°K.

The magnetic field at the nucleus due to orbital motion of electrons at the bottom of a non-degenerate band is given by Yafet[26] to be

$$\Delta H_d = (4\pi - D) \cdot \chi_d \cdot H \tag{41}$$

where χ_d is the diamagnetic susceptibility tensor, D is the demagnetizing coefficient tensor, and H is the applied magnetic field. The tensor χ_d will have a term which is independent of H and a term which oscillates as H is varied. These two terms will be superimposed on the paramagnetic term which gives rise to the Knight shift. Stephen[27] has calculated the oscillatory part of the shielding factor, $\sigma_d = 4\pi \chi_d$, and has found it to be

$$(42)\ \sigma_d(\text{osc}) = -\frac{12N\pi^3\mu_o^{*}kT}{V\,\zeta_o\,H}\cdot\sum_{n=1}^{\infty}(-1)^n I(n)\cos\left(n\pi\frac{m^*}{m}\right)\frac{\sin\left(\frac{n\pi\,\zeta_o}{\mu_o^{*}H}\right)}{\sinh\left(\frac{n\pi^2 kT}{\mu_o^{*}H}\right)}$$

where $\frac{N}{V}$ is the density of electrons involved in this interaction

m^* is the effective mass of the electron

μ_o^* is the "effective" Bohr magneton (m^* replaces m)

ζ_o is the Fermi energy

$I(n)$ is an integral to be evaluated numerically

k is Boltzmann's constant

T is temperature

As can be seen from equation (42), $\sigma_d(\text{osc})$ varies periodically in $\frac{1}{H}$. Further, since m^* depends on the orientation of the Fermi surface, that is the crystal orientation in the magnetic field, the $\sin\left(\frac{n\pi\zeta_o}{\mu_o^{*}H}\right)$ factor means σ_d (osc) will be anisotropic. For comparatively low fields such as 10 kilogauss, where $\frac{\zeta_o}{\mu_o^{*}H} \approx 500$, this anisotropy would completely mask any effect in a powder whose particles are randomly oriented in the magnetic field.

For fields of the order of 10 kilogauss and for liquid helium temperatures, the amplitude of the first term

of equation (42) is

$$(43) \qquad \left[\sigma_d(\text{osc})\right]_{\max} = \frac{12N\pi}{V\zeta_o} \frac{\mu_o^{*2} I(1)}{}$$

where Stephen gives I(1) a value of about .1. If we substitute in suitable values for the parameters, we find that $\frac{\Delta H_d}{H}$ is of the order of 10^{-6} for both aluminum and tin. This is less than one percent of the Knight shift and would be an upper limit to the effect since D has been assumed to be zero. The period of the oscillations is given by $\Delta\left(\frac{n\pi\zeta_o}{\mu_o^* H}\right) = 2\pi$. Using the experimental value for the periods of aluminum and tin given by Shoenberg[22], we find that at 10 kilogauss aluminum has a period of about 30 gauss and tin has one between 20 gauss and 60 gauss, depending on the crystal orientation in the magnetic field.

Because the theory for these diamagnetic oscillations in the Knight shift is at best only an order of magnitude theory, it was felt worthwhile to search for them in spite of their small predicted amplitude. The measurements were all done at 1.5°K at fields near 10 kilogauss. The method of recording the data to ensure greatest possible accuracy has already been described in Chapter 3. Signals were recorded at intervals of a few gauss over a range of magnetic field corresponding to at least one period. The

results of the experiments are shown in Figures 11 and 12. Within the accuracy of the experiment, neither the aluminum nor tin crystal gave any indication of these diamagnetic oscillations. An upper limit to their contribution to the Knight shift was found to be about .002% for the aluminum crystal and .001% for the tin crystal.

Similar experiments were attempted on a bismuth single crystal which should have a much greater amplitude of σ_d(osc) than either tin or aluminum. However, no signal from bismuth was observed at liquid helium temperatures, probably because of the long relaxation time of bismuth[26].

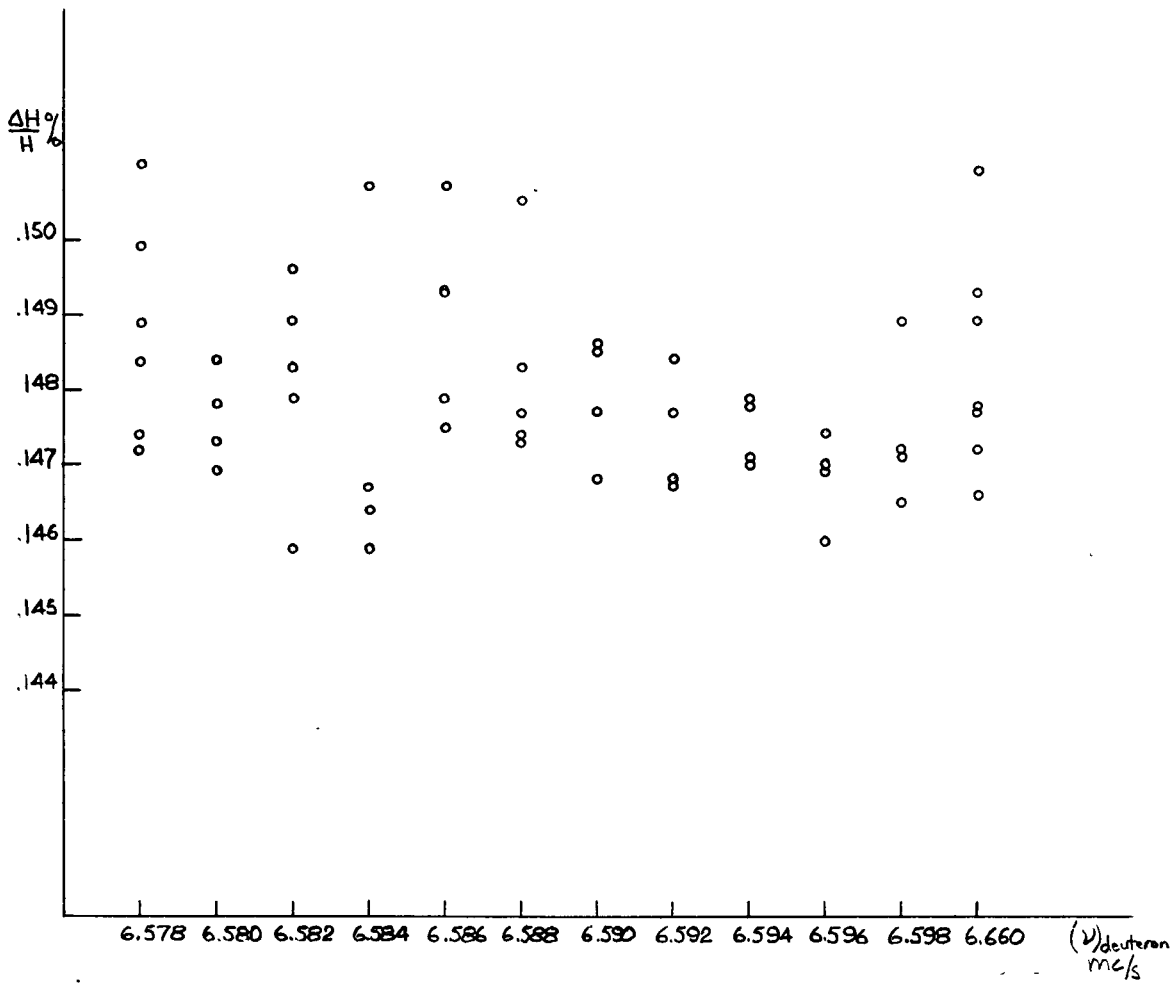

Figure 11. The Knight Shift in Aluminum as a Function of Magnetic Field
(Magnetic field measured in terms of the deuteron resonance)

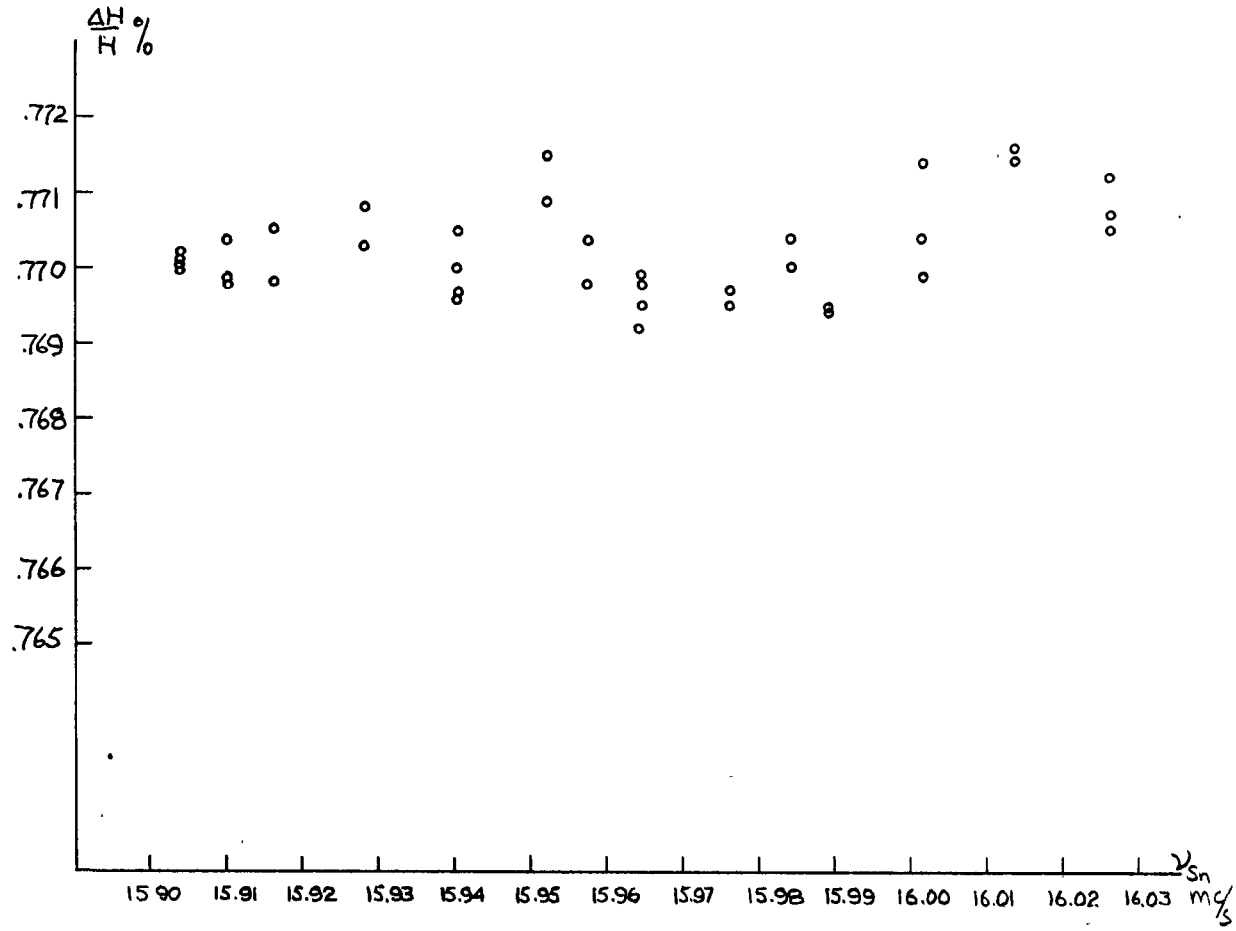

Figure 12. The Knight Shift in Tin as a Function of Magnetic Field
(Magnetic field measured in terms of the non-metal Sn resonance)

APPENDIX A

THE SECOND MOMENT OF THE RESONANCE LINE DUE TO MISALIGNMENT OF THE CRYSTAL SLICES

The resonance frequency in a single crystal with tetragonal symmetry measured from its average value $\nu_0(1+K)$ is

$$\nu = \tfrac{1}{2} \Delta \nu_{\parallel}' \ (3 \cos^2 \theta - 1)$$

where $\Delta \nu_{\parallel}' = K_{\parallel}' \nu_0$. This equation follows from equation (32). We assume that the slices are misaligned such that θ varies between $\theta_0 - \alpha$ and $\theta_0 + \alpha$, where α is a measure of the misalignment of the crystal slices. To calculate the second moment of the absorption signal due to misalignment, we consider the following quantities. The average value of ν is defined by

$$\overline{\nu} = \int \nu \, f(\nu) \, d\nu$$

where $f(\nu) \, d\nu$ is the probability that the resonance frequency is between ν and $\nu + d\nu$. If we assume an

isotropic distribution in θ between the two limits $\theta_o - \alpha$ and $\theta_o + \alpha$, then

$$f(u)du = \frac{du}{b-a} = \frac{1}{b-a}\,\frac{du}{d\nu}\,d\nu = f(\nu)\,d\nu$$

where $u = \cos\theta$, $b = \cos(\theta_o - \alpha)$, and $a = \cos(\theta_o + \alpha)$. Thus $\overline{\nu}$ can be written

$$\overline{\nu} = \frac{\Delta\nu_{\parallel}'}{2} \int_a^b \frac{(3u^2 - 1)}{b - a}\,du$$

$$= \frac{\Delta\nu_{\parallel}'}{2}\,(b^2 + ba + a^2 - 1)$$

Similarly $\overline{\nu 2}$ can be written

$$\overline{\nu^2} = \left(\frac{\Delta\nu_{\parallel}'}{2}\right)^2 \int_a^b \frac{(9u^4 - 6u^2 + 1)}{b - a}\,du$$

$$= \left(\frac{\Delta\nu_{\parallel}'}{2}\right)^2 \left\{\frac{9}{5}\,(b^4 + b^3a + a^2b^2 + ba^3 + a^4) - 2(b^2 + ba + a^2) + 1\right\}$$

The second moment due to misalignment of the crystal slices is

$$\overline{(v - \bar{v})^2} = \overline{v^2} - (\bar{v})^2$$

$$= \left(\frac{\Delta v_{\parallel}'}{2}\right)^2 \left\{\frac{4}{5}(b^4 + a^4) - \frac{1}{5}(b^3a + b^2a^2 + ba^3)\right\}$$

If $b = \cos(\theta - \alpha)$ and $a = \cos(\theta + \alpha)$, then

$$\overline{v^2} - (\bar{v})^2 = \left(\frac{\Delta v_{\parallel}'}{2}\right)^2 \left\{12 \cos^2\theta \cos^2\alpha \sin^2\theta \sin^2\alpha + \frac{4}{5} \sin^4\theta \sin^4\alpha\right\}$$

THE ANISOTROPY OF THE NUCLEAR MAGNETIC RESONANCE IN WHITE TIN *

E. P. JONES ** and D. LLEWELYN WILLIAMS ***
Department of Physics, University of British Columbia,
Vancouver 8, B.C., Canada

Received 17 April 1962

The nuclear magnetic resonance signal in white tin has been studied in some detail in the powder [1-3], and it has been established that the observed broad line is a consequence of the anisotropy of the Knight shift in tin together with the effect of nuclear spin exchange between different isotopes [4]. Bloembergen and Rowland [5], from observations on thallium, have suggested that the exchange interaction need not be isotropic.

In the hope of clarifying these ideas, a direct study of the anisotropy of both the Knight shift and the line width has been carried out in a single crystal specimen of white tin. The specimen was constructed in the form of a multiple layer sandwich of 0.1 mm thick oriented in tin layers separated by 0.05 mm layers of Mylar; the whole cemented together with a silicone resin spray. The tin layers were formed by etching down 1 mm thick tin slices cut from a single crystal.

The signals were observed with a Pound-Knight spectrometer, and in view of the comparatively weak tin signal, measurements were taken at the lowest available temperature (~ 1.15°K). A steady magnetic field of 10 kilogauss was produced by a Varian 12 inch rotatable magnet and was monitored by the deuteron resonance in D_2O. Rotations were performed in the mutually perpendicular planes shown in fig. 1. The observed anisotropy in the Knight shift and in the line width determined by the maxima in the derivative of the Sn^{119} resonance are shown in figs. 2 and 3. The anisotropy was checked for 180° symmetry by two points at 225° and 315°.

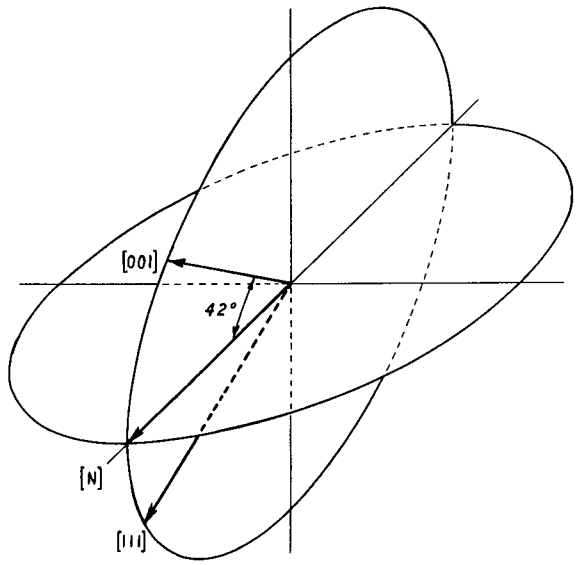

Fig. 1. The $(1\bar{1}0)$ plane containing the [001] and the [111] directions, and the plane perpendicular to it. The magnetic field is rotated in either of these planes.

The Knight shift is closely expressible in terms

* Research supported by the National Research Council of Canada.
** Holder of International Nickel Company of Canada Research Fellowship.
*** National Research Council of Canada Postdoctoral Fellow.

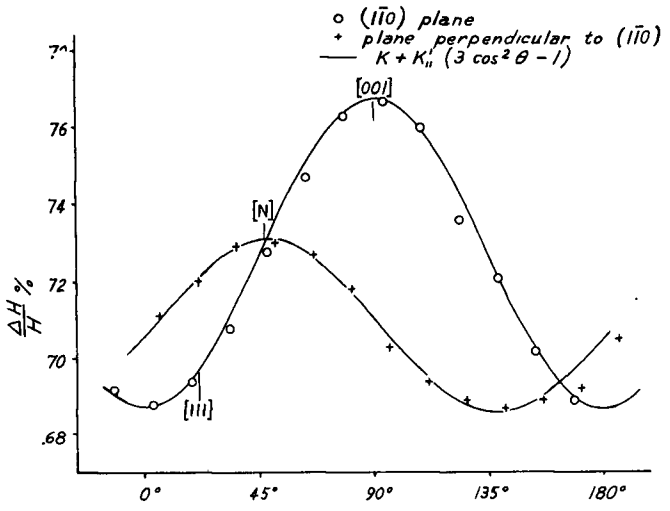

Fig. 2. The Sn^{119} Knight shift as a function of crystal orientation in the magnetic field.

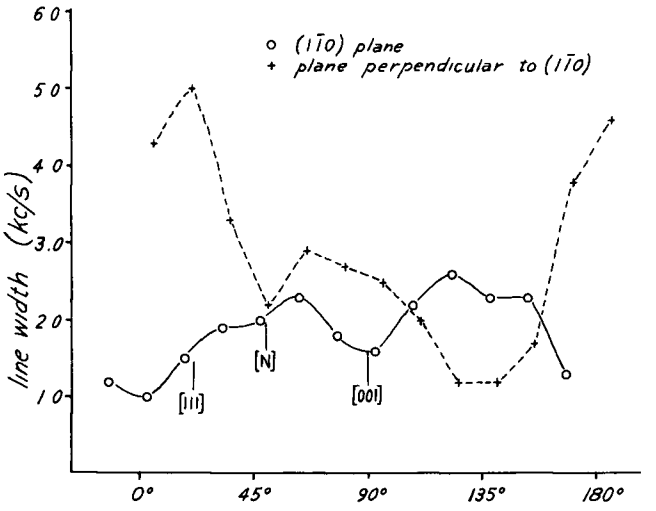

Fig. 3. The Sn^{119} line width as a function of crystal orientation in the magnetic field.

of the expected relation for tetragonal symmetry [6]

$$\frac{\Delta H}{H} = K + \tfrac{1}{2} K'_{\parallel} (3\cos^2\theta - 1) ,$$

where θ is the angle between the magnetic field and the (001) axis. Our results are compared with other values in table 1.

Table 1. Knight shift constants.

	$K \times 10^4$	$K'_{\parallel} \times 10^4$
Ref. [1]	70.9 ± 0.7	
Ref. [2]	75.7	2.3
Ref. [3]	-	6.6 ± 0.6
Present experiment	71.3 ± 0.2	5.4 ± 0.2

The anisotropy of the line width differs in both form and magnitude from that expected from dipolar broadening alone. The mean value is in agreement with that of Karimov and Shchegolev for the second moment (1.2 (kc/s)^2) and if the additional broadening is attributed to the exchange interaction, this interaction has a large anisotropic component. A detailed expression for this is available [5] and calculations on the implications of the observed anisotropy are in progress.

In these experiments the sample size is much greater than the electromagnetic skin-depth. Theory [7] indicates that the line-shape should then be an equal mixture of absorption and dispersion modes. No obvious contribution from the dispersion mode was observed, in agreement with previous observations [3,8] that there seems to be an effective skin-depth for nuclear magnetic resonance which is greater than the electromagnetic skin-depth. In any case, such a mixing would increase our value of K by only one percent and would have a negligible effect on $K'_{\parallel}$.

One can readily understand errors in an analysis of the powder line shape since a weighting factor corresponding to the anisotropy of the line width should be used. This factor probably explains most of the discrepancy between the results quoted in table 1.

The observed line-shape showed some asymmetry which appeared to be a function of orientation. Work is continuing on a detailed investigation of these points together with a study of the Sn^{117} resonance.

We would like to thank Dr. E. Teghtsoonian and Mr. A. L. Causey for providing the tin single crystal and Dr. Myer Bloom for illuminating discussions.

References

1) B.R.McGarvey and H.S.Gutowsky, J. Chem. Phys. 21 (1953) 2114.
2) N. Bloembergen and T.J.Rowland, Acta Met. 1 (1953) 731.
3) Yu.S.Karimov and I.F.Shchegolev, J. Exptl. Theoret. Phys. (USSR) 40 (1961) 1289; translation: Soviet Phys. JETP 13 (1961) 899.
4) M.A.Ruderman and C.Kittel, Phys. Rev. 96 (1954) 99.
5) N.Bloembergen and T.J.Rowland, Phys. Rev. 97 (1955) 1679.
6) A.Abragam, The principles of nuclear magnetism (Oxford University Press, 1961), p. 205.
7) A.C.Chapman, P.Rhodes and E.F.W.Seymour, Proc. Phys. Soc. (London) B 70 (1957) 345.
8) A.G.Redfield, Phys. Rev. 101 (1956) 67.

* * * * *

APPENDIX C

This appendix includes circuit diagrams of the non-commerical items of the spectrometer. One or two comments on the apparatus are appropriate.

The heaters of the Pound-Knight-Watkins oscillators and of the White amplifiers are supplied by a 6 volt storage battery in parallel with a Heathkit Battery Eliminator. A dc source for the heaters was found necessary especially for the White amplifiers to eliminate 60 c/s interference.

The Pound-Knight-Watkins oscillator used to measure the deuteron resonance employed a Varicap in the same way as shown in Figure C1, except that a 90 volt battery and a 100 K Helipot provided the voltage sweep instead of the modified Tektronix 162 waveform generator.

The initial voltage of the sweep of the modified Tektronix 162 waveform generator is set with the control marked Vernier, and the sawtooth run-down is begun or terminated with the switch marked Gate Out or Pulse Out. Figure C2 shows the modifications of the waveform generator in dotted squares. The rest of the circuit can be found in the Tektronix 162 waveform generator manual.

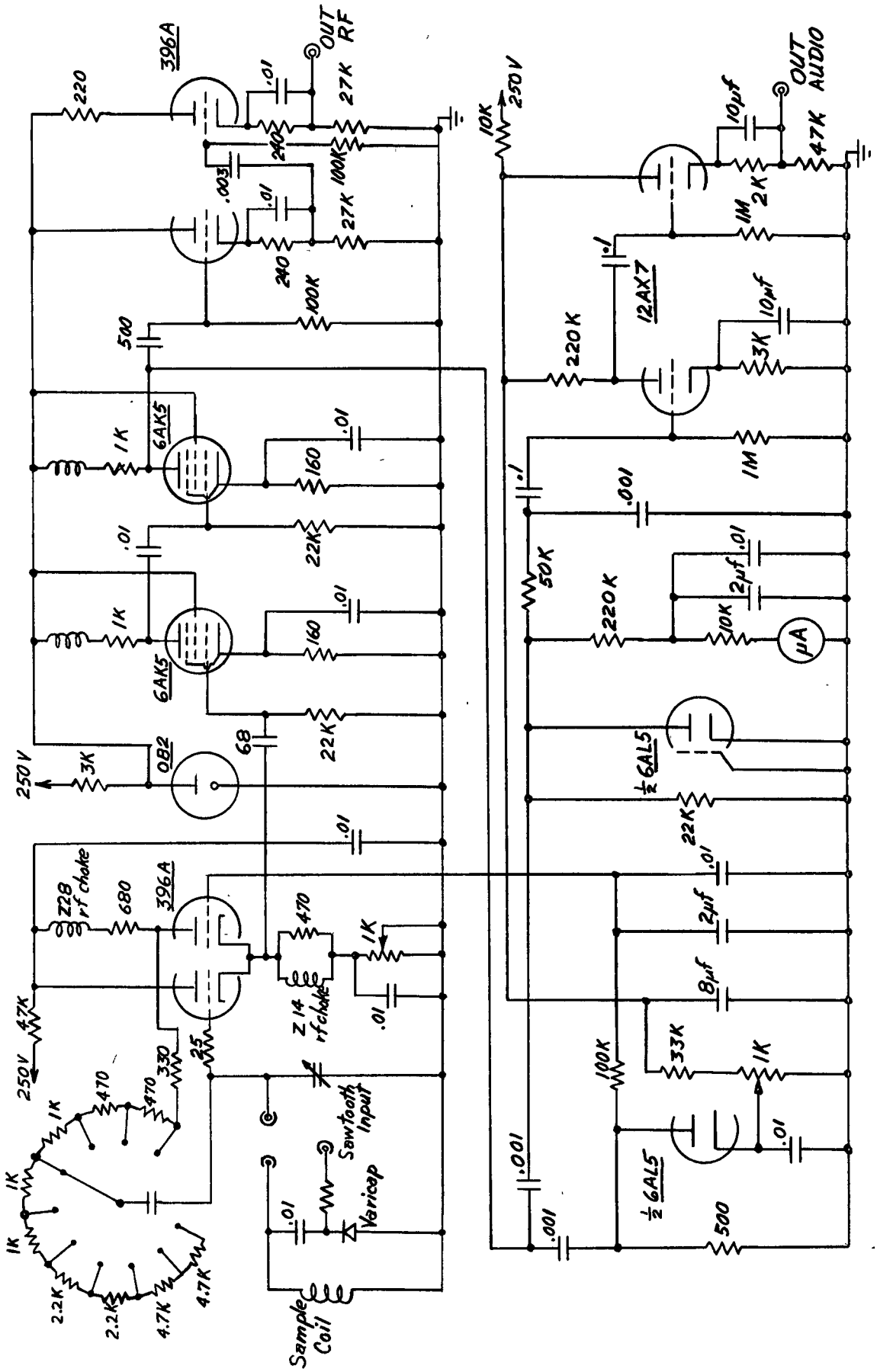

Figure C1. The Pound-Knight-Watkins Oscillator

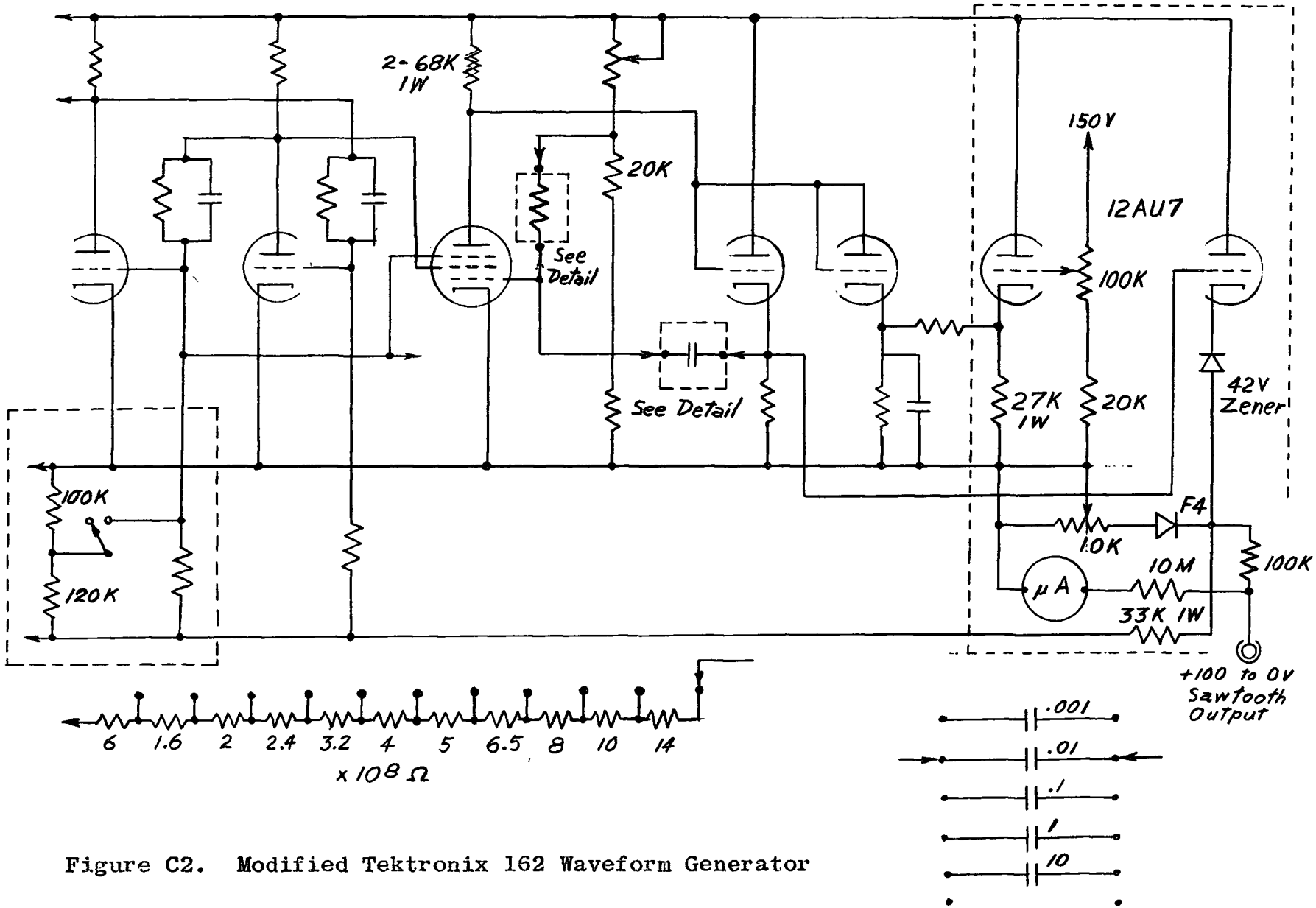

Figure C2. Modified Tektronix 162 Waveform Generator

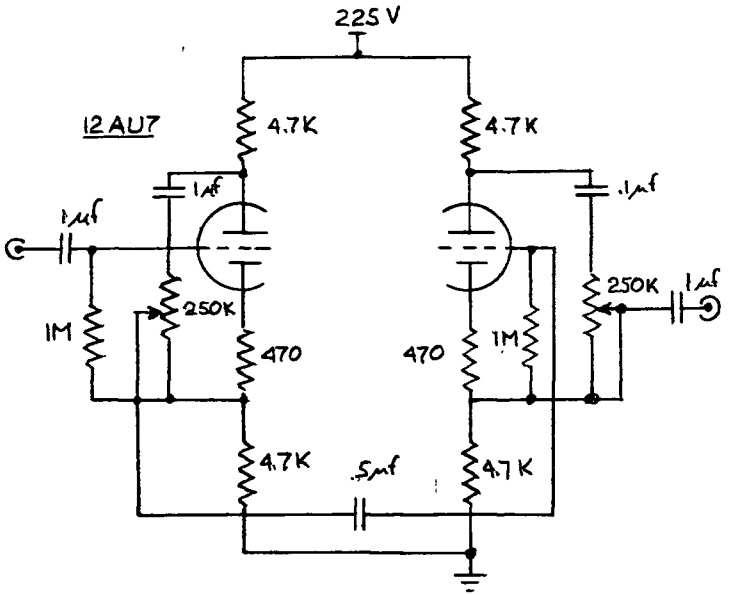

Phase Shifter

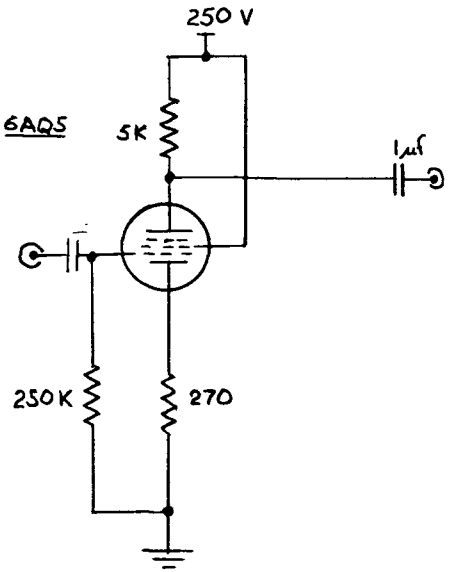

Horizontal Amplifier
for the Tektronix 360
Oscilloscope

Figure C3.

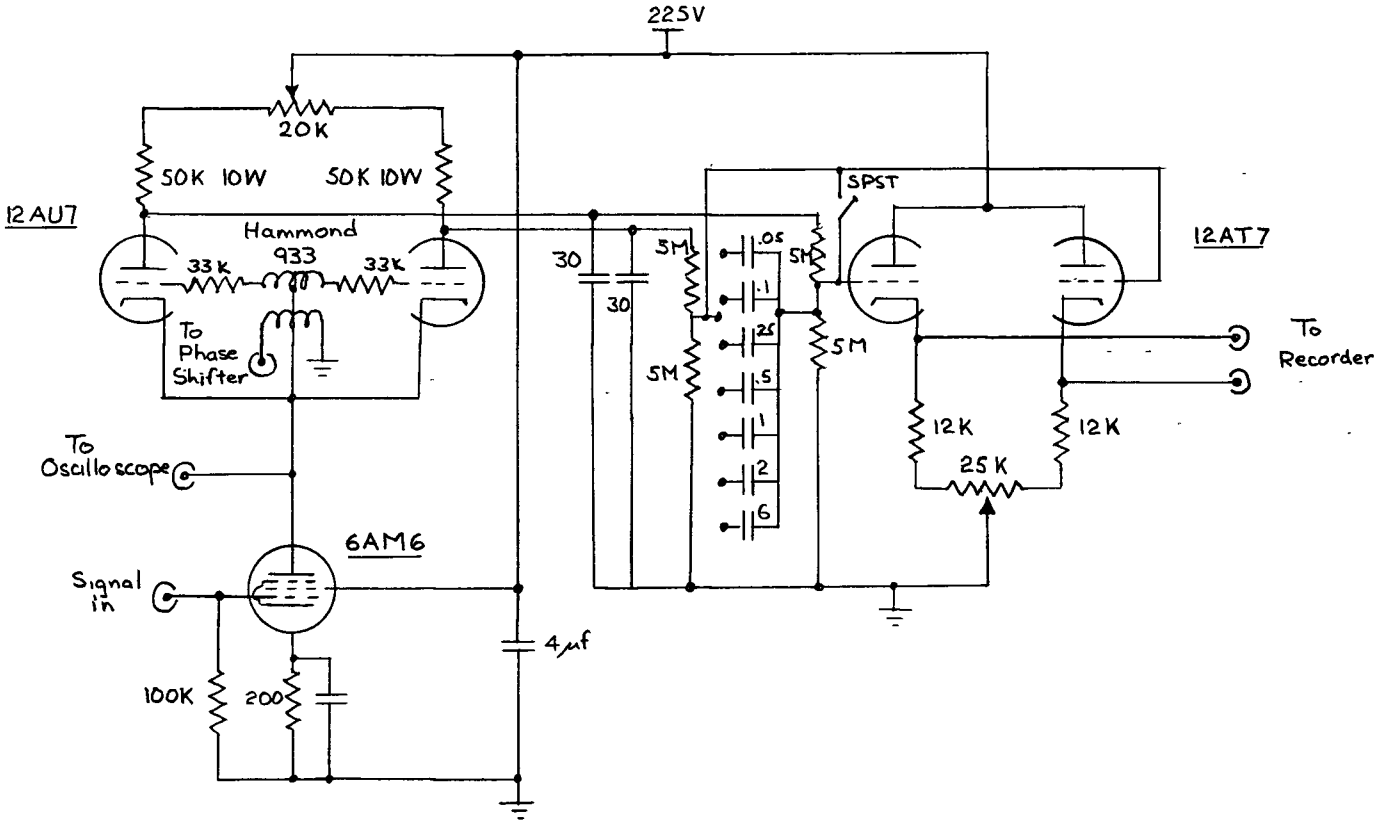

Figure C4. Phase Sensitive Detector

REFERENCES

1 C. H. Townes, C. Herring, W. D. Knight: Phys. Rev. 77 852 (1950)

2 W. D. Knight: Solid State Physics 2 93 (1956)

3 A. Abragam: The Principles of Nuclear Magnetism, Ch. IV

4 A. Abragam: The Principles of Nuclear Magnetism, p. 172

5 C. P. Slichter: Nuclear Magnetic Resonance, to be published

6 L. Pauling, E. B. Wilson: Introduction to Quantum Mechanics, p 232

7 N. Bloembergen, T. J. Rowland: Acta Met. 1 731 (1953)

8 A. Abragam: The Principles of Nuclear Magnetism, p 205

9 D. G. Watkins: Ph.D. Thesis, Harvard University (1952)

10 R. Blume: RSI 32 743 (1961)

11 E. Sawatzky: Ph.D. Thesis, University of B.C. (1961)

12 N. A. Shuster: RSI 22 254 (1951)

13 E. P. Jones, D. Ll. Williams: Physics Letters 1 109 (1962)

14 A. C. Chapman, P. Rhodes, E. F. W. Seymour: Proc. Phys. Soc. B LXX 345 (1957)

15 Yu. S. Karimov, I. F. Shchegolev: JETP (USSR) 40 1289 (1961), transl: JETP 13 899 (1961)

16 J. H. Van Vleck: Phys. Rev. 74 1168 (1948)

17 M. A. Ruderman, C. Kittel: Phys. Rev. 96 99 (1954)

18 N. Bloembergen, T. J. Rowland: Phys. Rev. 97 1679 (1955)

19 A. Abragam: The Principles of Nuclear Magnetism, p 207

20 A. V. Gold, M. J. Priestly: Phil. Mag. 5 1089 (1960)

21 S. Tolansky, G. O. Forester: Phil. Mag. 32 315 (1941)

22 D. Shoenberg: Progress in Low Temperature Physics II, p 226

23 R. G. Chambers: Can. J. Phys. 34 1395 (1956)

24 A. B. Pippard: Reports on Progress in Physics 22 176 (1960)

25 T. P. Das, E. H. Sondheimer: Phil. Mag. 5 529 (1960)

26 Y. Yafet: J. Phys. Chem. Solids 21 99 (1961)

27 M. J. Stephen: Phys. Rev. 123 126 (1961)

28 J. I. Kaplan: J. Phys. Chem. Solids 23 826 (1962)

29 M. J. Stephen: Proc. Phys. Soc. 79 987 (1962)

30 J. E. Hebborn, M. J. Stephen: Proc. Phys. Soc. 80 991 (1962)

31 P. L. Sagalyn, J. A. Hofmann: Bull. APS, Ser. II 7 226 (1962)
Phys. Rev. 127 68 (1962)